EUROPEAN ORGANISATION FOR NUCLEAR RESEARCH (CERN)

Submitted to: Nucl. Phys. B

CERN-PH-EP-2015-288
13th June 2016

arXiv:1512.02913v2 [hep-ex] 10 Jun 2016

source: https://doi.org/10.7892/boris.99987 | downloaded: 5.5.2023

Measurement of $D^{*\pm}$, $D^{\pm}$ and $D_s^{\pm}$ meson production cross sections in pp collisions at $\sqrt{s} = 7$ TeV with the ATLAS detector

The ATLAS Collaboration

Abstract

The production of $D^{*\pm}$, $D^{\pm}$ and $D_s^{\pm}$ charmed mesons has been measured with the ATLAS detector in pp collisions at $\sqrt{s} = 7$ TeV at the LHC, using data corresponding to an integrated luminosity of $280\,\text{nb}^{-1}$. The charmed mesons have been reconstructed in the range of transverse momentum $3.5 < p_{\text{T}}(D) < 100$ GeV and pseudorapidity $|\eta(D)| < 2.1$. The differential cross sections as a function of transverse momentum and pseudorapidity were measured for $D^{*\pm}$ and $D^{\pm}$ production. The next-to-leading-order QCD predictions are consistent with the data in the visible kinematic region within the large theoretical uncertainties. Using the visible D cross sections and an extrapolation to the full kinematic phase space, the strangeness-suppression factor in charm fragmentation, the fraction of charged non-strange D mesons produced in a vector state, and the total cross section of charm production at $\sqrt{s} = 7$ TeV were derived.

© 2016 CERN for the benefit of the ATLAS Collaboration.
Reproduction of this article or parts of it is allowed as specified in the CC-BY-4.0 license.

Contents

1 Introduction

Measurements of heavy-quark production at the Large Hadron Collider (LHC) provide a means to test perturbative quantum chromodynamics (QCD) calculations at the highest available collision energies. Since the current calculations suffer from large theoretical uncertainties, the experimental constraints on heavy-quark production cross sections are important for measurements in the electroweak and Higgs sectors, and in searches for new physics phenomena, for which heavy-quark production is often an important background process.

Charmed mesons are produced in the hadronisation of charm and bottom quarks, which are copiously produced in pp collisions at $\sqrt{s} = 7$ TeV. The ATLAS detector[1] [1] at the LHC has been used previously to measure D^{*+} mesons[2] produced in jets [2] and in bottom hadron decays in association with muons [3]. Associated production of D mesons and W bosons has been also studied by the ATLAS collaboration [4].

[1] The ATLAS coordinate system is a Cartesian right-handed system, with the coordinate origin at the nominal interaction point. The anti-clockwise beam direction defines the positive z-axis, with the x-axis pointing to the centre of the LHC ring. Polar (θ) and azimuthal (ϕ) angles are measured with respect to this reference system, which corresponds to the centre-of-mass frame of the colliding protons. The pseudorapidity is defined as $\eta = -\ln\tan(\theta/2)$ and the transverse momentum is defined as $p_{\mathrm{T}} = p\sin\theta$. The rapidity is defined as $y = 0.5\ln((E + p_z)/(E - p_z))$, where E and p_z refer to energy and longitudinal momentum, respectively.

[2] Hereafter, charge conjugation is implied.

Production of D mesons in the hadronisation of charm quarks has been studied by the ALICE collaboration in the central rapidity range ($|y| < 0.5$) [5, 6] and by the LHCb collaboration at forward rapidities ($2.0 < y < 4.5$) [7]. Open-charm production was also measured by the CDF collaboration [8] at the Tevatron collider in $p\bar{p}$ collisions at $\sqrt{s} = 1.96\,\text{TeV}$.

In this paper, measurements of the inclusive D^{*+}, D^+ and D_s^+ production cross sections and their comparison with next-to-leading-order (NLO) QCD calculations are presented. Contributions from both charm hadronisation and bottom hadron decays have been included in the measured visible D production cross sections and in the NLO QCD predictions. The measured visible cross sections have been extrapolated to the cross sections for D meson production in charm hadronisation in the full kinematic phase space, after subtraction of the cross-section fractions originating from bottom production. The extrapolated cross sections have been used to calculate the total cross section of charm production in pp collisions at $\sqrt{s} = 7\,\text{TeV}$ and two fragmentation ratios for charged charmed mesons: the strangeness-suppression factor and the fraction of charged non-strange D mesons produced in a vector state.

2 The ATLAS detector

A detailed description of the ATLAS detector can be found elsewhere [1]. A brief outline of the components most relevant to this analysis is given below.

The ATLAS inner detector has full coverage in ϕ, covers the pseudorapidity range $|\eta| < 2.5$ and operates inside an axial magnetic field of 2 T of a superconducting solenoid. It consists of a silicon pixel detector (Pixel), a silicon microstrip detector (semiconductor tracker, SCT) and a transition radiation tracker (TRT). The inner-detector barrel (end-cap) parts consist of 3 (2×3) Pixel layers, 4 (2×9) double-layers of single-sided SCT strips and 73 (2×160) layers of TRT straws. The TRT straws enable track-following up to $|\eta| = 2.0$.

The calorimeter system is placed outside the solenoid. A high-resolution liquid-argon electromagnetic sampling calorimeter covers the pseudorapidity range $|\eta| < 3.2$. This calorimeter is complemented by hadronic calorimeters, built using scintillating tiles in the range $|\eta| < 1.7$ and liquid-argon technology in the end-cap ($1.5 < |\eta| < 3.2$). Forward calorimeters extend the coverage to $|\eta| < 4.9$.

The ATLAS detector has a three-level trigger system [9]. For the measurement of D mesons with $3.5 < p_{\text{T}} < 20$ GeV (low-p_{T} range), two complementary minimum-bias triggers are used. The first trigger relies on the first-level trigger signals from the Minimum Bias Trigger Scintillators (MBTS). The MBTS are mounted at each end of the inner detector in front of the liquid-argon end-cap calorimeter cryostats at $z = \pm 3.56\,\text{m}$ and are segmented into eight sectors in azimuth and two rings in pseudorapidity ($2.09 < |\eta| < 2.82$ and $2.82 < |\eta| < 3.84$). The MBTS trigger used in this analysis is configured to require at least one hit above threshold. The second minimum-bias trigger uses the inner detector at the second-level trigger to select inelastic events on randomly chosen bunch crossings (Random). For D mesons with $20 < p_{\text{T}} < 100$ GeV (high-p_{T} range), the first-level calorimeter-based jet triggers are used. The jet triggers use coarse detector information to identify areas in the calorimeter with energy deposits above certain thresholds. A simplified jet-finding algorithm based on a sliding window of configurable size is used to trigger events. The algorithm uses towers with a granularity of $\Delta\phi \times \Delta\eta = 0.2 \times 0.2$ as inputs. In this paper, the first-level jet triggers with energy thresholds of 5, 10 and 15 GeV are used. No further jet selection requirements are applied at the second and third trigger levels.

The integrated luminosity is calculated by measuring interaction rates using several ATLAS devices at small angles to the beam direction, with the absolute calibration obtained from beam-separation scans. The uncertainty of the luminosity measurement for the event sample used in this analysis is estimated to be 3.5% [10].

3 Event simulation

To model inelastic events produced in pp collisions, a large sample of Monte Carlo (MC) simulated events is prepared using the PYTHIA 6.4 [11] MC generator. The simulation is performed using leading-order matrix elements for all $2 \to 2$ QCD processes. Initial- and final-state parton showering is used to simulate the effect of higher-order processes. The MRST LO* [12] parameterisation is used for the parton distribution functions (PDF) of the proton. The charm- and bottom-quark masses are set to 1.5 GeV and 4.8 GeV, respectively. The event sample is generated using the ATLAS AMBT1 set of tuned parameters [13]. The fraction of the D meson sample produced in bottom-hadron decays (~10%) is normalised using the measured production cross section of b-hadrons decaying to $D^{*+}\mu^{-}X$ final states [3].

The generated events are passed through a full ATLAS detector simulation [14] based on GEANT4 [15, 16] and processed with the same reconstruction program as used for the data.

4 QCD calculations

The measured D cross sections are compared with the fixed-order next-to-leading-logarithm (FONLL) [17–19] predictions, with the general-mass variable-flavour-number scheme (GM-VFNS) [20–22] calculations and with the NLO QCD calculations matched with a leading-logarithm parton-shower MC simulation (NLO-MC). A web interface was used to obtain up-to-date FONLL predictions [23], while the GM-VFNS predictions have been provided by their authors. Two methods are presently available for performing the NLO-MC matched calculations: MC@NLO [24] and POWHEG [25]. Their implementations in the codes MC@NLO 3.42 [26] and POWHEG-hvq 1.01 [27] are used. MC@NLO 3.42 is matched with the HERWIG 6.5 [28] MC event generator, while POWHEG-hvq 1.01 is used with both HERWIG 6.5 and PYTHIA 6.4.

The main differences between the GM-VFNS and the other calculations considered here originate from differences between the so-called massless and massive schemes. In the massive scheme, the heavy quark Q appears only in the final state and the $m_Q^2/p_{\mathrm{T},Q}^2$ power terms of the perturbative series are correctly accounted for, where $p_{\mathrm{T},Q}$ is the transverse momentum of the heavy quark and m_Q is its pole mass. The massive-scheme calculations are not reliable for $p_{\mathrm{T},Q} \gg m_Q$ due to neglected terms of the type $\ln(p_{\mathrm{T},Q}^2/m_Q^2)$. In the massless scheme, the heavy quark occurs as an initial-state parton and the large logarithmic terms are absorbed into the heavy-quark contribution to the proton PDF, and into the fragmentation functions of the heavy-quark transition to a hadron. The massless calculations are reliable only for $p_{\mathrm{T},Q} \gg m_Q$ due to the assumption that $m_Q = 0$. The FONLL and GM-VFNS calculations were developed to obtain reliable predictions for $p_{\mathrm{T},Q} \approx m_Q$. In FONLL, the massive and massless predictions are matched exactly up to $O(\alpha_s^3)$, and spurious higher-order terms with potentially unphysical behaviour are damped using a weighting function. The FONLL parton cross sections are convolved with non-perturbative fragmentation functions. GM-VFNS combines the massless predictions with the massive $m_Q^2/p_{\mathrm{T},Q}^2$ power terms and derives subtraction terms by comparing the massive and massless

cross sections in the limit $m_Q \to 0$. The large logarithmic terms in GM-VFNS remain absorbed in the PDF and in perturbatively evolved fragmentation functions with a non-perturbative input. Unlike other calculations, GM-VFNS considers fragmentation to D mesons from light quarks and gluons in addition to the heavy-quark fragmentation [29].

All predictions are obtained using the CTEQ6.6 [30] parameterisation for the proton PDF. The value of the QCD coupling constant is set to $\alpha_s(m_Z) = 0.118$ in accord with the central CTEQ6.6 analysis. Both the charm and bottom contributions to the charmed meson production cross sections are included in all predictions. The charm-quark pole mass is set to 1.5 GeV in all calculations. The bottom-quark pole mass is set to 4.75 GeV in the FONLL, MC@NLO and POWHEG calculations. In the GM-VFNS calculations, the bottom-quark pole mass is set to 4.5 GeV. The renormalisation and factorisation scales are set to $\mu_r = \mu_f = \mu$, where μ is defined as

$$\mu^2 = m_Q^2 + p_{\mathrm{T},Q}^2$$

in the FONLL and GM-VFNS calculations. For MC@NLO,

$$\mu^2 = m_Q^2 + \frac{(p_{\mathrm{T},Q} + p_{\mathrm{T},\bar{Q}})^2}{4},$$

where $p_{\mathrm{T},Q}$ and $p_{\mathrm{T},\bar{Q}}$ are the transverse momenta of the produced heavy quark and antiquark, respectively, and m_Q is the heavy-quark pole mass. For POWHEG,

$$\mu^2 = m_Q^2 + (m_{Q\bar{Q}}^2/4 - m_Q^2) \cdot \sin^2(\theta_Q),$$

where $m_{Q\bar{Q}}$ is the invariant mass of the produced $Q\bar{Q}$ system and θ_Q is the polar angle of the heavy quark in the $Q\bar{Q}$ system centre-of-mass frame.

The specific FONLL fragmentation functions [23, 31] as well as the GM-VFNS fragmentation functions [29] were obtained using e^+e^- data. In the case of the NLO-MC matched calculations, the heavy-quark hadronisation is performed using the cluster model [32] when interfaced to HERWIG. When interfaced to PYTHIA, the Lund string model [33] with the Bowler modification [34] of the Lund symmetric fragmentation function [35] for heavy quarks is used.

In the FONLL, MC@NLO and POWHEG calculations, the fragmentation fractions of heavy quarks hadronising as a particular charmed meson, $f(Q \to D)$, are set to experimental values obtained by averaging the LEP measurements in hadronic Z decays [36]. They are summarised in Table 1. In GM-VFNS, the fragmentation fractions of heavy quarks, light quarks and gluons were obtained using e^+e^- data, along with the fragmentation functions [29].

The following sources of theoretical uncertainty are considered for the FONLL, MC@NLO and POWHEG predictions:

- Scale uncertainty. The uncertainty was determined by varying μ_r and μ_f independently to $\mu/2$ and 2μ, with the additional constraint $1/2 < \mu_r/\mu_f < 2$, and selecting the largest positive and negative variations.
- Pole-mass uncertainty. The uncertainty is determined by varying the charm- and bottom-quark masses independently by ± 0.2 GeV and ± 0.25 GeV, respectively. The total m_Q uncertainty is obtained by adding in quadrature separately the positive and negative cross-section variations.

	LEP data
$f(c \to D^{*+})$	$0.236 \pm 0.006 \pm 0.003$
$f(c \to D^{+})$	$0.225 \pm 0.010 \pm 0.005$
$f(c \to D_s^{+})$	$0.092 \pm 0.008 \pm 0.005$
$f(b \to D^{*\pm})$	$0.221 \pm 0.009 \pm 0.003$
$f(b \to D^{\pm})$	$0.223 \pm 0.011 \pm 0.005$
$f(b \to D_s^{\pm})$	$0.138 \pm 0.009 \pm 0.006$

Table 1: The fractions of c and b quarks hadronising as a particular charmed meson, $f(Q \to D)$, obtained by averaging the LEP measurements [36]. The first uncertainties are the combined statistical and systematic uncertainties of the measurements. The second uncertainties originate from uncertainties in the relevant branching fractions.

- PDF uncertainty. The uncertainty is determined by using the CTEQ6.6 PDF error eigenvectors. For MC@NLO and POWHEG, the PDF α_s uncertainties are also calculated using eigenvectors for ± 0.002 variations of α_s. Following the PDF4LHC recommendations [37], the CTEQ6.6 PDF and PDF α_s uncertainties, provided at 90% confidence level (CL), are scaled to 68% CL. The total PDF uncertainty (for FONLL) or the combined PDF and α_s (PDF$\oplus\alpha_s$) uncertainty (for MC@NLO and POWHEG) is obtained by adding in quadrature separately the positive and negative cross-section variations.
- Fragmentation-fraction uncertainty. The uncertainty is the combined statistical and systematic uncertainty of the LEP measurements [36]. The uncertainties on the fragmentation fractions originating from uncertainties in the relevant branching fractions are not included because they affect experimental and theoretical cross-section calculations in the same way and can be ignored in the comparison.

For the POWHEG+PYTHIA predictions, the hadronisation uncertainty for each D meson is obtained as a sum in quadrature of the corresponding fragmentation-fraction uncertainty and the fragmentation-function uncertainty. The latter uncertainty is determined by using the Peterson fragmentation function [38] with extreme choices [39–43] of the fragmentation parameter: 0.02 and 0.1 for charm fragmentation, and 0.002 and 0.01 for bottom fragmentation.

Only the scale uncertainty, which is dominant, is calculated for GM-VFNS by varying three scale parameters: the renormalisation scale, the factorisation scale for initial-state singularities and the factorisation scale for final-state singularities. These three scales are varied independently to $\mu/2$ and 2μ, with the additional constraint for the ratio of any two scales to be between $1/2$ and 2, and the largest positive and negative variations are selected.

5 Event selection

The data used in this analysis were collected in 2010 with the ATLAS detector in pp collisions at $\sqrt{s} = 7$ TeV at the LHC. The crossing angle of the colliding protons was either zero or negligible in the rapidity range of the measurement. To measure D mesons with $p_{\mathrm{T}} < 20$ GeV, the events collected

with the minimum-bias MBTS and Random triggers are used; these triggers are unbiased for the events of interest [9]. However, the rate from the triggers exceeded the allotted trigger bandwidth after the initial data-taking period and thus prescale factors were applied to reduce the output rate. Taking into account the prescale factors, the data sample corresponds to an integrated luminosity of $1.04\,\text{nb}^{-1}$. To measure D mesons in the intervals $20 < p_{\text{T}} < 30$ GeV, $30 < p_{\text{T}} < 40$ GeV and $40 < p_{\text{T}} < 100$ GeV, the first-level jet triggers with energy thresholds of 5, 10 and 15 GeV, respectively, are used. The trigger efficiencies for the corresponding D meson p_{T} ranges are above 90%. The efficiencies are derived from the MC simulation. The simulation uncertainties are estimated from data–MC comparisons using independent trigger selections with softer thresholds on the jet energy or energy in the electromagnetic calorimeter. The triggers with energy thresholds of 5 and 10 GeV were prescaled during some parts of the data-taking period; their corresponding integrated luminosities are $28\,\text{nb}^{-1}$ and $90\,\text{nb}^{-1}$, respectively. The data sample taken with the unprescaled jet trigger with the energy threshold of 15 GeV corresponds to an integrated luminosity of $280\,\text{nb}^{-1}$.

The event samples are processed using the standard offline ATLAS detector calibration and event reconstruction [1,44]. Only events with at least three reconstructed tracks with $p_{\text{T}} > 100$ MeV and at least one reconstructed primary-vertex candidate [45] are kept for the reconstruction of charmed mesons.

6 Reconstruction of charmed mesons

The D^{*+}, D^+ and D_s^+ charmed mesons are reconstructed in the range of transverse momentum $3.5 < p_{\text{T}}(D) < 100$ GeV and pseudorapidity $|\eta(D)| < 2.1$. As no significant differences between results for positively and negatively charged charmed mesons are observed, all results are presented for the combined samples.

Charmed meson candidates are reconstructed using tracks measured in the inner tracking detector. To ensure high reconstruction efficiency and good momentum resolution, each track is required to satisfy $|\eta| < 2.5$, have at least one hit in the Pixel detector and at least four hits in the SCT. The $\text{d}E/\text{d}x$ particle identification with the Pixel detector [46] is not used since it is not effective in the kinematic ranges utilised for the charmed-meson reconstruction.

There can be several primary-vertex candidates in an event due to multiple collisions per bunch crossing. To identify the heavy-quark production vertex, requirements on the D meson transverse impact parameter, d_0, and longitudinal impact parameter, z_0, with respect to the primary-vertex candidate are imposed. In the rare case ($< 1\%$) that more than one vertex satisfies these requirements, the hard-scatter primary vertex is taken to be the one with the largest sum of the squared transverse momenta of its associated tracks.

For D mesons with momenta in the low-p_{T} range, the background from non-signal track combinations (combinatorial background) is significantly reduced by requiring $p_{\text{T}}(D^{*+}, D^+, D_s^+)/\sum p_{\text{T}}(\text{track}) > 0.05$, where $\sum p_{\text{T}}(\text{track})$ is the scalar sum of the transverse momenta of all tracks associated with the primary vertex. MC studies indicate that due to properties of heavy-quark fragmentation, more than 99% of D signals satisfy this selection criterion. Further background rejection is achieved by imposing requirements on the D^0 (from the $D^{*+} \to D^0\pi^+$ decay), D^+ and D_s^+ transverse decay lengths[3] with respect to the primary vertex, L_{xy}, and on the transverse momenta and decay angles of the charmed meson decay products.

[3] The transverse decay length of a particle is the transverse distance between the primary or production vertex and the particle decay vertex, projected along the transverse momentum of the particle.

The requirement values are tuned using the MC simulation to enhance signal-to-background ratios while keeping acceptances high.

The details of the reconstruction for each of the three charmed meson samples are given in the next subsections.

6.1 Reconstruction of D^{*+} mesons

The D^{*+} mesons are identified using the decay $D^{*+} \to D^0\pi_s^+ \to (K^-\pi^+)\pi_s^+$. The pion from the $D^{*+} \to D^0\pi^+$ decay is referred to as the "soft" pion, π_s^+, because its momentum is limited by the small mass difference between the D^{*+} and D^0.

In each event, pairs of tracks from oppositely charged particles, each with $p_{\mathrm{T}} > 1$ GeV, are combined to form D^0 candidates. Any additional track, with $p_{\mathrm{T}} > 0.25$ GeV, is combined with the D^0 candidate to form a D^{*+} candidate. The three tracks of the D^{*+} candidate are fitted using a constraint on the $D^{*+} \to D^0\pi_s^+ \to (K^-\pi^+)\pi_s^+$ topology, i.e. the two tracks of the D^0 candidate are required to intersect at a single vertex and the D^0 trajectory is required to intersect with the third track, producing the D^{*+} vertex. To calculate the D^0 candidate invariant mass, $m(K\pi)$, kaon and pion masses are assumed in turn for each track. The additional track is assigned the pion mass and this pion is required to have a charge opposite to that of the kaon. The mass $m(K\pi)$, the three-particle invariant mass $m(K\pi\pi_s)$, and the mass difference, $\Delta m = m(K\pi\pi_s) - m(K\pi)$, are calculated using the track momenta refitted to the decay topology. To suppress combinatorial background the following requirements are used:

- $\chi^2 < 25$, where χ^2 is the D^{*+} candidate fit quality. The requirement value is loose as the signal-to-background ratio decreases rather slowly with χ^2.
- $|d_0(D^{*+})| < 0.5$ mm.
- $|z_0(D^{*+}) \sin\theta(D^{*+})| < 0.5$ mm.
- $L_{xy}(D^0) > 0.1$ mm.
- $|\cos\theta^*(K)| < 0.95$, where $\theta^*(K)$ is the angle between the kaon in the $K\pi$ rest frame and the $K\pi$ line of flight in the laboratory frame.

Figure 1 shows the Δm distributions for low-p_{T} and high-p_{T} D^{*+} candidates with $m(K\pi)$ values consistent with the world average D^0 mass [47]. To take the mass resolution into account, the selection requirement is varied from $1.83 < m(K\pi) < 1.90$ GeV for the D^{*+} candidates with small $|\eta|$ and p_{T} values to $1.78 < m(K\pi) < 1.95$ GeV for the D^{*+} candidates with large $|\eta|$ and p_{T} values. Sizeable signals are seen around the world average value of $m(D^{*+}) - m(D^0) = 145.4527 \pm 0.0017$ MeV [47]. The dashed histograms show the distributions for wrong-charge combinations, in which both particles forming the D^0 candidate have the same charge and the third particle has the opposite charge. These distributions, which are quite similar to the distributions for right-charge combinations outside of the signal region, demonstrate the shapes of the combinatorial background components. The Δm distributions for the right-charge combinations outside of the signal region are slightly above those for the wrong-charge combinations due to contributions from neutral-meson decays to two particles with opposite charges, in particular due to the contribution from D^0 mesons not originating from $D^{*+} \to D^0\pi^+$ decays.

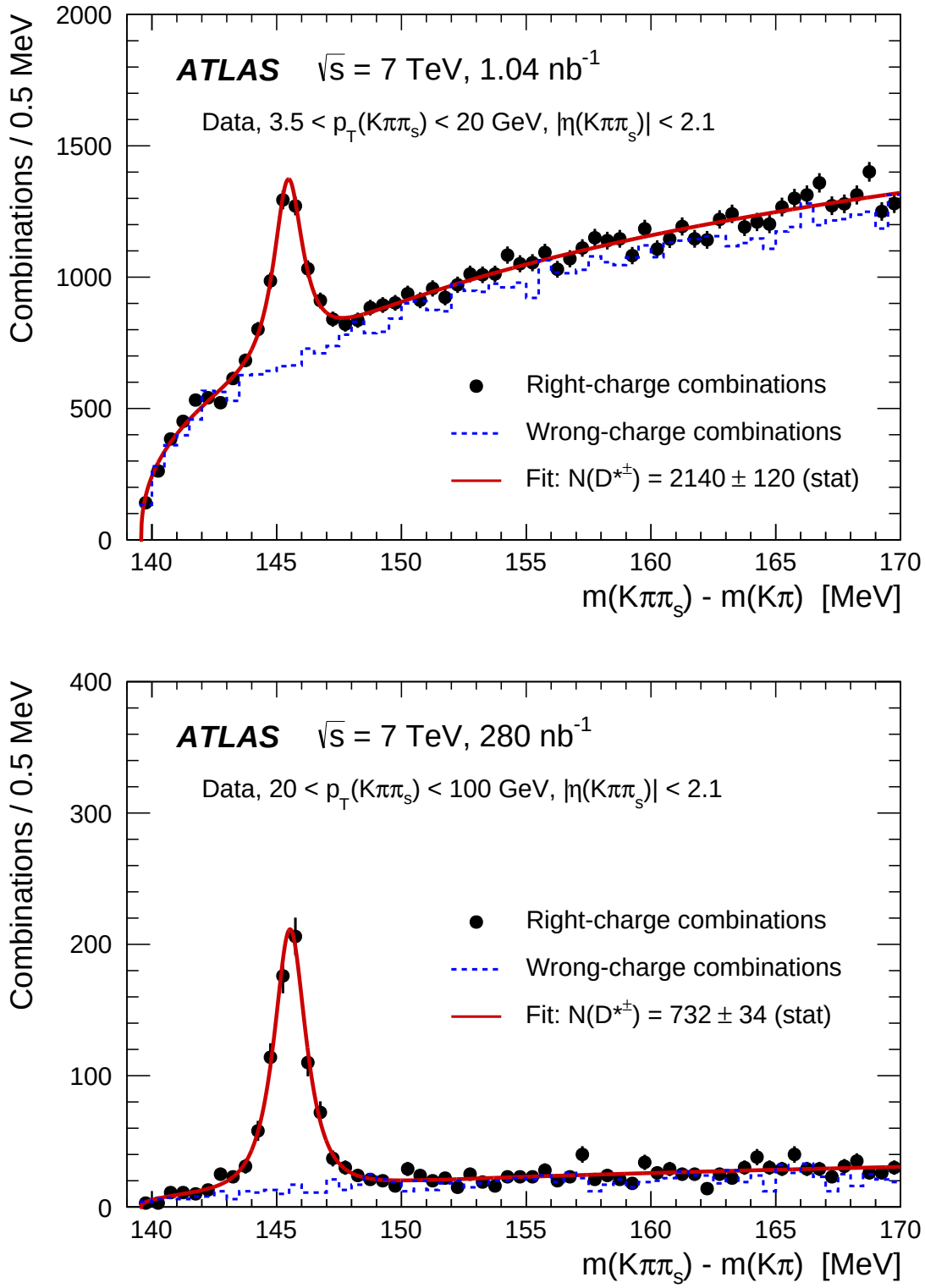

Figure 1: The distribution of the mass difference, $\Delta m = m(K\pi\pi_s) - m(K\pi)$, for $D^{*\pm}$ candidates with $3.5 < p_{\mathrm{T}}(D^{*\pm}) < 20$ GeV (top) and $20 < p_{\mathrm{T}}(D^{*\pm}) < 100$ GeV (bottom). The data are represented by the points with error bars (statistical only). The dashed histograms show the distributions for wrong-charge combinations. The solid curves represent fit results (see text).

The Δm distributions are fitted to the sum of a modified Gaussian function [48] describing the signal and a threshold function describing the non-resonant background. The modified Gaussian function is defined as

$$\text{Gauss}^{\text{mod}} \propto \exp[-0.5 \cdot x^{1+1/(1+0.5\cdot x)}],$$

where $x = |(\Delta m - m_0)/\sigma|$. This functional form, introduced to take into account the non-Gaussian tails of resonant signals, describes both the data and MC signals well. The signal position, m_0, and width, σ, as well as the number of D^{*+} mesons are free parameters of the fit. The threshold function has the form $A \cdot (\Delta m - m_{\pi^+})^B \cdot \exp[C \cdot (\Delta m - m_{\pi^+}) + D \cdot (\Delta m - m_{\pi^+})^2]$, where m_{π^+} is the pion mass and A, B, C and D are free parameters. The fitted $D^{*\pm}$ yields are $N(D^{*\pm}) = 2140 \pm 120\,(\text{stat})$ and $N(D^{*\pm}) = 732 \pm 34\,(\text{stat})$ for the low-p_{T} and high-p_{T} ranges, respectively. Small admixtures ($< 1\%$) to the reconstructed signals from the $D^{*+} \to D^0\pi^+$ decays with D^0 decays to final states other than $K^-\pi^+$ are taken into account in the acceptance correction procedure (Section 7). The combined value of the fitted mass differences is $145.47 \pm 0.03\,(\text{stat})$ MeV, in agreement with the world average. The widths of the signals are ~0.6 MeV, in agreement with the MC expectations.

6.2 Reconstruction of D^+ mesons

The D^+ mesons are reconstructed from the decay $D^+ \to K^-\pi^+\pi^+$. In each event, two tracks from same-charge particles each with $p_{\text{T}} > 0.8$ GeV are combined with a track from the opposite-charge particle with $p_{\text{T}} > 1$ GeV to form a D^+ candidate. At least one of the two particles with the same charge is required to have $p_{\text{T}} > 1$ GeV. Only three-track combinations successfully fitted to a common vertex are kept. The pion mass is assigned to each of the two tracks from same-charge particles and the kaon mass is assigned to the third track, after which the candidate invariant mass, $m(K\pi\pi)$, is calculated using the track momenta refitted to the common vertex. To suppress combinatorial background the following requirements are used:

- $\chi^2 < 12$, where χ^2 is the D^+ candidate vertex fit quality.
- $|d_0(D^+)| < 0.15$ mm.
- $|z_0(D^+)\sin\theta(D^+)| < 0.3$ mm.
- $L_{xy}(D^+) > 1.2$ mm. The large value of the requirement on $L_{xy}(D^+)$ is motivated by the relatively large lifetime of the D^+ meson [47] and the large combinatorial background.
- $\cos\theta^*(K) > -0.8$, where $\theta^*(K)$ is the angle between the kaon in the $K\pi\pi$ rest frame and the $K\pi\pi$ line of flight in the laboratory frame.
- $\cos\theta^*(\pi) > -0.85$, where $\theta^*(\pi)$ is the angle between the pion in the $K\pi\pi$ rest frame and the $K\pi\pi$ line of flight in the laboratory frame.

To suppress background from D^{*+} decays, combinations with $m(K\pi\pi) - m(K\pi) < 153$ MeV are removed. The background from $D_s^+ \to \phi\pi^+$, with $\phi \to K^+K^-$, is suppressed by rejecting any three-track D^+ candidate comprised of a pair of tracks of oppositely charged particles which, when assuming the kaon mass for both tracks, has a two-track invariant mass within ±8 MeV of the world average ϕ mass [47]. MC studies indicate that the suppression of the $D^{*+} \to D^0\pi^+$ decays has a negligible effect on the D^+ signal, and the suppression of the $D_s^+ \to \phi\pi^+$ decays rejects less than 2% of the signal. The remaining small background from $D_s^+ \to K^+K^-\pi^+$ decays is subtracted using the simulated reflection shape normalised to the measured D_s^+ rate (Section 6.3). Smaller contributions, affecting mass ranges outside the expected

D^+ signal, from the decays $D_s^+ \to \pi^+\pi^-\pi^+$, $D^+ \to K^+K^-\pi^+$, $D^+ \to \pi^+\pi^-\pi^+$ and $D^+ \to \pi^+\pi^-\pi^+\pi^0$ are subtracted using the simulated reflection shapes normalised to the measured D^+ and D_s^+ rates.

Figure 2 shows the $m(K\pi\pi)$ distributions for low-$p_{\rm T}$ and high-$p_{\rm T}$ D^+ candidates after all requirements. Sizeable signals are seen around the world average value of the D^+ mass, 1869.61 ± 0.10 MeV [47]. The mass distributions are fitted to the sum of a modified Gaussian function describing the signal and a quadratic exponential function describing the non-resonant background. The quadratic exponential function has the form $A \cdot \exp(B \cdot m + C \cdot m^2)$, where A, B and C are free parameters. The fitted $D^\pm$ yields are $N(D^\pm) = 1990 \pm 100\,(\text{stat})$ and $N(D^\pm) = 1730 \pm 100\,(\text{stat})$ for the low-$p_{\rm T}$ and high-$p_{\rm T}$ ranges, respectively. The combined D^+ mass value is $1870.0 \pm 0.7\,(\text{stat})$ MeV, in agreement with the world average. The widths of the signals are ∼15 MeV, in agreement with the MC expectations.

6.3 Reconstruction of D_s^+ mesons

The D_s^+ mesons are reconstructed from the decay $D_s^+ \to \phi\pi^+$ with $\phi \to K^+K^-$. In each event, tracks from particles with opposite charges and $p_{\rm T} > 1$ GeV are assigned the kaon mass and combined in pairs to form ϕ candidates. Any additional track with $p_{\rm T} > 1$ GeV is assigned the pion mass and combined with the ϕ candidate to form a D_s^+ candidate. Only three-track combinations successfully fitted to a common vertex are kept. The ϕ candidate invariant mass, $m(KK)$, and the D_s^+ candidate invariant mass, $m(KK\pi)$, are calculated using the track momenta refitted to the common vertex. To suppress combinatorial background the following requirements are used:

- $\chi^2 < 12$, where χ^2 is the D_s^+ candidate vertex fit quality.
- $|d_0(D_s^+)| < 0.15$ mm.
- $|z_0(D_s^+)\sin\theta(D_s^+)| < 0.3$ mm.
- $L_{xy}(D_s^+) > 0.4$ mm.
- $-0.8 < \cos\theta^*(\pi) < 0.7$, where $\theta^*(\pi)$ is the angle between the pion in the $KK\pi$ rest frame and the $KK\pi$ line of flight in the laboratory frame.
- $|\cos^3\theta'(K)| > 0.2$, where $\theta'(K)$ is the angle between either of the kaons and the pion in the KK rest frame. The decay of the pseudoscalar D_s^+ meson to the ϕ (vector) plus π^+ (pseudoscalar) final state results in an alignment of the spin of the ϕ meson transverse to the direction of motion of the ϕ relative to the D_s^+. Consequently, the distribution of $\cos\theta'(K)$ follows a $\cos^2\theta'(K)$ shape, implying a uniform distribution for $\cos^3\theta'(K)$. In contrast, the $\cos\theta'(K)$ distribution of the combinatorial background is uniform and its $\cos^3\theta'(K)$ distribution peaks at zero. The requirement suppresses the background significantly while reducing the signal by 20%.

Small contributions, affecting mass ranges outside the expected D_s^+ signal, from the decays $D_s^+ \to \phi K^+$, $D_s^+ \to \phi\pi^+\pi^0$, $D^+ \to \phi\pi^+\pi^0$ and $D^+ \to K^-\pi^+\pi^+$ are subtracted using the simulated reflection shapes normalised to the measured D^+ and D_s^+ rates.

Figure 3 shows the $m(KK\pi)$ distributions for low-$p_{\rm T}$ and high-$p_{\rm T}$ D_s^+ candidates with $m(KK)$ within ±7 MeV of the world average ϕ mass [47]. Sizeable signals are seen around the world average value of the D_s^+ mass, 1968.30 ± 0.11 MeV [47]. Smaller signals are visible around the world average value of $m(D^+)$, as expected from the decay $D^+ \to \phi\pi^+$ with $\phi \to K^+K^-$.

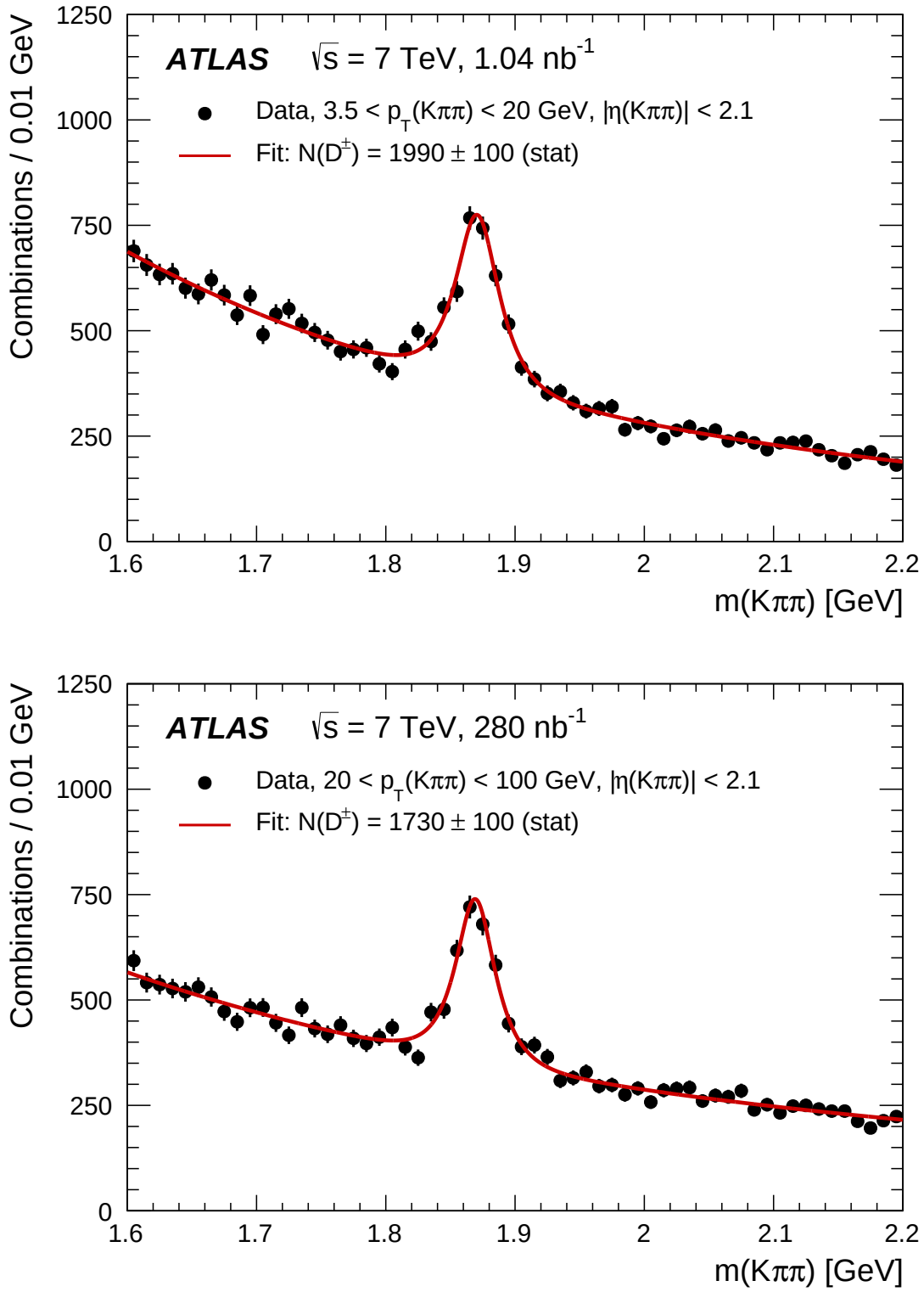

Figure 2: The $m(K\pi\pi)$ distributions for $D^{\pm}$ candidates with $3.5 < p_{\mathrm{T}}(D^{\pm}) < 20$ GeV (top) and $20 < p_{\mathrm{T}}(D^{\pm}) < 100$ GeV (bottom). The data are represented by the points with error bars (statistical only). The solid curves represent fit results (see text).

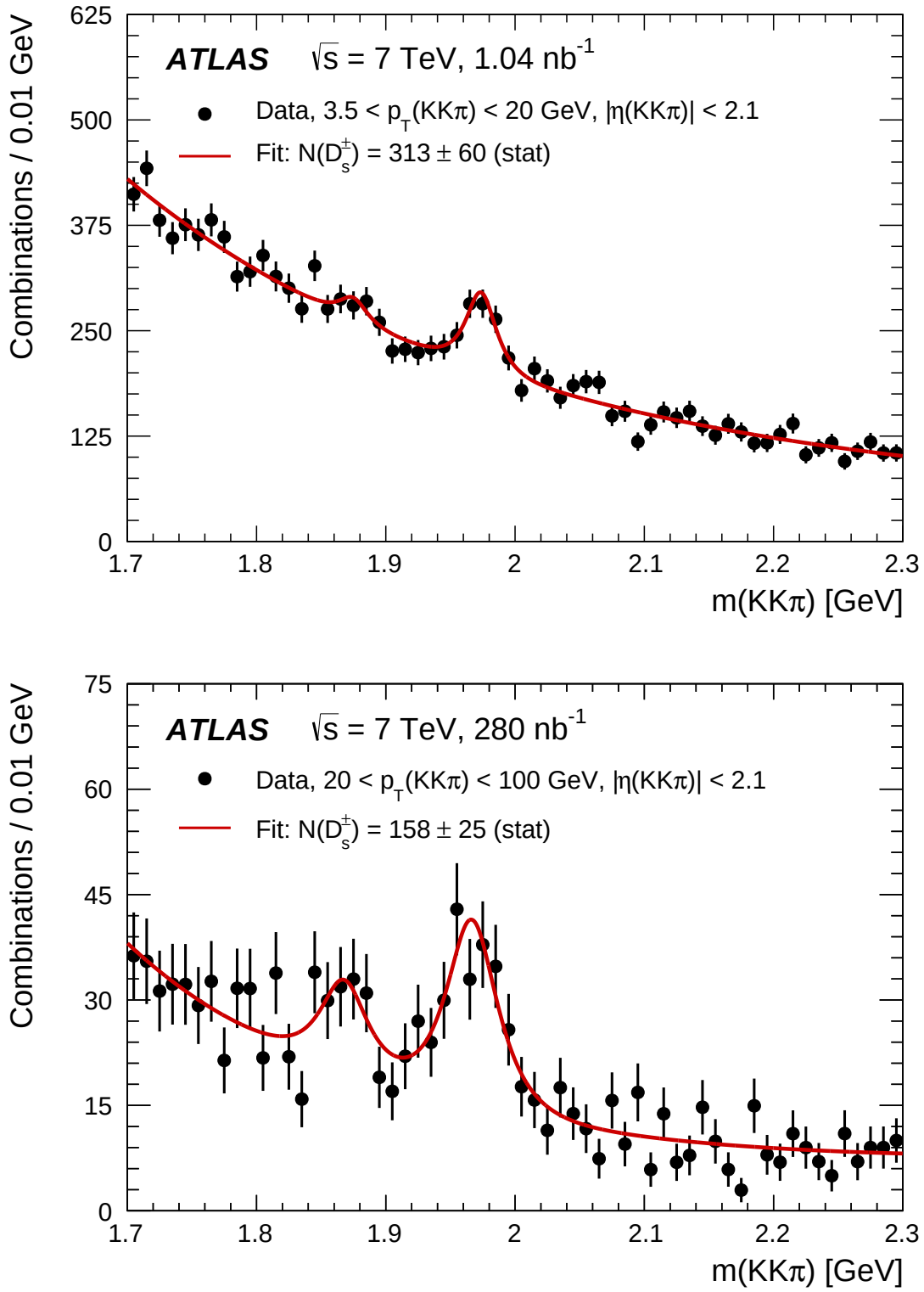

Figure 3: The $m(KK\pi)$ distributions for $D_s^{\pm}$ candidates with $3.5 < p_{\mathrm{T}}(D_s^{\pm}) < 20$ GeV (top) and $20 < p_{\mathrm{T}}(D_s^{\pm}) < 100$ GeV (bottom). Small signals visible around the world average value of $m(D^+)$ are from the decay $D^+ \to \phi\pi^+$ with $\phi \to K^+K^-$. The data are represented by the points with error bars (statistical only). The solid curves represent the fit results (see text).

The $m(KK\pi)$ distributions are fitted to the sum of two modified Gaussian functions describing the D_s^+ and D^+ signals and a quadratic exponential function describing the non-resonant background. For the small D^+ signals, the signal positions are fixed to the D_s^+ signal positions minus the world average value of $m(D_s^+) - m(D^+)$ [47], and their widths are fixed using the D_s^+ signal widths and the MC ratio of the D^+ and D_s^+ widths. The fitted $D_s^\pm$ yields are $N(D_s^\pm) = 313 \pm 60\,(\text{stat})$ and $N(D_s^\pm) = 158 \pm 25\,(\text{stat})$ for the low-p_T and high-p_T ranges, respectively. The combined D_s^+ mass value is $1971.2 \pm 2.0\,(\text{stat})$ MeV, in agreement with the world average. The widths of the signals are ~15 MeV, in agreement with the MC expectations.

7 Data correction and systematic uncertainties

The visible D production cross sections are measured for the process $pp \to DX$ in the kinematic region $3.5 < p_\text{T}(D) < 100$ GeV and $|\eta(D)| < 2.1$. The cross section for a given charmed meson is calculated in the low-p_T range, $3.5 < p_\text{T}(D) < 20$ GeV, and high-p_T range, $20 < p_\text{T}(D) < 100$ GeV, from

$$\sigma_{pp\to DX} = \frac{N(D)}{\mathcal{A} \cdot \mathcal{L} \cdot \mathcal{B}}\,, \tag{1}$$

where $N(D)$ is the number of reconstructed charmed mesons with positive and negative charges, $\mathcal{A}$ is the reconstruction acceptance obtained from the MC sample, $\mathcal{L}$ is the integrated luminosity and $\mathcal{B}$ is the branching fraction or the product of the branching fractions for the decay channel used in the reconstruction. The reconstruction acceptance takes into account efficiencies, migrations and small remaining admixtures in the reconstructed signals from other decay modes. To calculate the D^{*+} and D^+ production cross sections, the world average $\mathcal{B}$ values [47] are used. For D_s^+, the measurement by the CLEO experiment [49] of the partial $D_s^+ \to K^+K^-\pi^+$ branching fractions, with a kaon-pair mass within various intervals around the world average ϕ meson mass, is used. Interpolating between the partial branching fractions, measured for the ±5 MeV and ±10 MeV intervals, yields the value $(1.85 \pm 0.11)\%$ for the ±7 MeV interval used in this analysis.

The differential cross sections $\mathrm{d}\sigma/\mathrm{d}p_\text{T}$ and $\mathrm{d}\sigma/\mathrm{d}|\eta|$ are calculated for D^{*+} and D^+ production[4] in nine bins in p_T ($3.5-5;\ 5-6.5;\ 6.5-8;\ 8-12;\ 12-20;\ 20-30;\ 30-40;\ 40-60;\ 60-100$ GeV), and five bins in $|\eta|$ ($0-0.2;\ 0.2-0.5;\ 0.5-0.8;\ 0.8-1.3;\ 1.3-2.1$) for both the low-$p_\text{T}$ and high-p_T ranges. To obtain the differential cross section in a given bin, the visible cross section in the bin is divided by the bin width. The numbers of D^{*+} and D^+ mesons in each bin are obtained using the same procedure as that described in Section 6.

The following groups of systematic uncertainty sources are considered:

- $\{\delta_1\}$ The uncertainty of the jet trigger efficiencies. It is estimated using data–MC comparisons with independent trigger selections.
- $\{\delta_2\}$ The uncertainty of the track reconstruction and selection [13]. It is dominated by the uncertainty on the description of the detector material in the MC simulation. The uncertainty is calculated taking into account the p_T and η distributions of the D decay products.

[4] For D_s^+ production, the differential cross sections are not calculated due to insufficient sample size.

- $\{\delta_3\}$ The uncertainty of the D meson selection efficiency. It is determined by varying the MC reconstruction resolutions for the variables used in the selection of the D meson by amounts reflecting possible differences between the data and MC. For the $p_{\mathrm{T}}(D^{*+}, D^+, D_s^+)/\sum p_{\mathrm{T}}(\mathrm{track}) > 0.05$ requirement, the uncertainty is determined by repeating all calculations without this requirement.
- $\{\delta_4\}$ The uncertainty related to the D signal extraction procedures. It is determined by varying the background parameterisations and the ranges used for the signal fits. In addition, in the D^+ signal extraction procedure, the normalisation of the subtracted $D_s^+ \to K^-K^+\pi^+$ reflection is varied in the combined range of the normalisation statistical uncertainty and normalisation uncertainty propagated from the branching fraction uncertainties [47]. In the D_s^+ signal extraction procedure, the constraints used for the small D^+ signals are varied in the ranges of the MC statistical uncertainty for the ratio of the D^+ and D_s^+ widths and the uncertainty of world average value of $m(D_s^+) - m(D^+)$ [47].
- $\{\delta_5\}$ The model dependence of the acceptance corrections. It is obtained by varying in the MC simulation:
  - the $p_{\mathrm{T}}(D)$ and $|\eta(D)|$ distributions while preserving agreement with the data distributions,
  - the relative beauty contribution in the range allowed by the b-hadron cross-section measurement [3],
  - the lifetimes of charmed (D^+, D^0, D_s^+) and beauty (B^+, B^0, B_s^0, Λ_b^0) hadrons in the ranges of their uncertainties [47].
- $\{\delta_6\}$ The uncertainty of the acceptance corrections related to the MC statistical uncertainty.
- $\{\delta_7\}$ The uncertainty of the luminosity measurement [10].
- $\{\delta_8\}$ The uncertainty of the branching fractions [47, 49] used in Eq. (1).

Source	$\sigma^{\mathrm{vis}}(D^{*\pm})$		$\sigma^{\mathrm{vis}}(D^{\pm})$		$\sigma^{\mathrm{vis}}(D_s^{\pm})$	
	Low-p_{T}	High-p_{T}	Low-p_{T}	High-p_{T}	Low-p_{T}	High-p_{T}
Trigger (δ_1)	-	$^{+0.9}_{-1.0}\%$	-	$^{+0.9}_{-1.0}\%$	-	$^{+0.9}_{-1.0}\%$
Tracking (δ_2)	$\pm 7.8\%$	$\pm 7.4\%$	$\pm 7.7\%$	$\pm 7.4\%$	$\pm 7.6\%$	$\pm 7.4\%$
D selection (δ_3)	$^{+2.8}_{-1.6}\%$	$^{+1.7}_{-1.4}\%$	$^{+1.6}_{-1.0}\%$	$^{+0.9}_{-0.6}\%$	$^{+2.6}_{-1.6}\%$	$^{+1.1}_{-0.9}\%$
Signal fit (δ_4)	$\pm 1.3\%$	$\pm 0.9\%$	$\pm 1.3\%$	$\pm 1.5\%$	$\pm 6.4\%$	$\pm 5.3\%$
Modelling (δ_5)	$^{+1.0}_{-1.7}\%$	$^{+2.7}_{-2.3}\%$	$^{+2.3}_{-2.6}\%$	$^{+2.9}_{-2.4}\%$	$^{+1.7}_{-2.4}\%$	$^{+2.8}_{-2.4}\%$
Size of MC sample (δ_6)	$\pm 0.6\%$	$\pm 0.9\%$	$\pm 0.8\%$	$\pm 0.8\%$	$\pm 2.9\%$	$\pm 3.1\%$
Luminosity (δ_7)	$\pm 3.5\%$	$\pm 3.5\%$	$\pm 3.5\%$	$\pm 3.5\%$	$\pm 3.5\%$	$\pm 3.5\%$
Branching fraction (δ_8)	$\pm 1.5\%$	$\pm 1.5\%$	$\pm 2.1\%$	$\pm 2.1\%$	$\pm 5.9\%$	$\pm 5.9\%$

Table 2: Systematic uncertainties for measurements of visible low-p_{T}, $3.5 < p_{\mathrm{T}}(D) < 20$ GeV, and high-p_{T}, $20 < p_{\mathrm{T}}(D) < 100$ GeV, cross sections of $D^{*\pm}$, $D^{\pm}$ and $D_s^{\pm}$ production with $|\eta| < 2.1$.

The systematic uncertainties are summarised in Table 2. Contributions from the systematic uncertainties $\delta_1 - \delta_6$, calculated for visible cross sections and all bins of the differential cross sections, are added in quadrature separately for positive and negative variations. Uncertainties linked with the luminosity measurement (δ_7) and branching fractions (δ_8) are quoted separately for the measured visible cross sections. For differential cross sections, the δ_7 and δ_8 uncertainties are not included in Tables 4–6 and Figs. 4–6.

8 Production cross sections of charmed mesons

The visible cross sections of D meson production in pp collisions at $\sqrt{s} = 7$ TeV for $|\eta(D)| < 2.1$ in the low-p_{T} range, $3.5 < p_{\mathrm{T}}(D) < 20$ GeV, are measured to be

$$\begin{aligned}
\sigma^{\mathrm{vis}}(D^{*\pm}) &= 331 \pm 18\,(\mathrm{stat}) \pm 28\,(\mathrm{syst}) \pm 12\,(\mathrm{lum}) \pm 5\,(\mathrm{br})\,\mu\mathrm{b}\,,\\
\sigma^{\mathrm{vis}}(D^{\pm}) &= 328 \pm 16\,(\mathrm{stat}) \pm 27\,(\mathrm{syst}) \pm 11\,(\mathrm{lum}) \pm 7\,(\mathrm{br})\,\mu\mathrm{b}\,,\\
\sigma^{\mathrm{vis}}(D_s^{\pm}) &= 160 \pm 31\,(\mathrm{stat}) \pm 17\,(\mathrm{syst}) \pm 6\,(\mathrm{lum}) \pm 10\,(\mathrm{br})\,\mu\mathrm{b}\,,
\end{aligned}$$

where the last two uncertainties are due to those on the luminosity measurement and the charmed meson decay branching fractions.

The POWHEG+PYTHIA predictions are

$$\begin{aligned}
\sigma^{\mathrm{vis}}(D^{*\pm}) &= 158^{+176}_{-81}\,(\mathrm{scale})^{+15}_{-16}\,(m_Q)^{+14}_{-13}\,(\mathrm{PDF}\oplus\alpha_s)^{+19}_{-16}\,(\mathrm{hadr})\,\mu\mathrm{b}\,,\\
\sigma^{\mathrm{vis}}(D^{\pm}) &= 134^{+145}_{-67}\,(\mathrm{scale})^{+12}_{-13}\,(m_Q)^{+12}_{-11}\,(\mathrm{PDF}\oplus\alpha_s)^{+21}_{-12}\,(\mathrm{hadr})\,\mu\mathrm{b}\,,\\
\sigma^{\mathrm{vis}}(D_s^{\pm}) &= 62^{+63}_{-29}\,(\mathrm{scale}) \pm 6\,(m_Q) \pm 5\,(\mathrm{PDF}\oplus\alpha_s)^{+7}_{-8}\,(\mathrm{hadr})\,\mu\mathrm{b}\,,
\end{aligned}$$

where the last uncertainty is due to that on hadronisation (see Section 4). The FONLL predictions for D^{*+} and D^+ are

$$\begin{aligned}
\sigma^{\mathrm{vis}}(D^{*\pm}) &= 202^{+119}_{-73}\,(\mathrm{scale})^{+36}_{-27}\,(m_Q) \pm 21\,(\mathrm{PDF}) \pm 5\,(\mathrm{ff})\,\mu\mathrm{b}\,,\\
\sigma^{\mathrm{vis}}(D^{\pm}) &= 174\ ^{+99}_{-60}\,(\mathrm{scale})^{+33}_{-24}\,(m_Q) \pm 18\,(\mathrm{PDF}) \pm 7\,(\mathrm{ff})\,\mu\mathrm{b}\,,
\end{aligned}$$

where the last uncertainty is due to that on the fragmentation function. The FONLL predictions for D_s^+ production are currently not available.

The visible cross sections of D meson production in pp collisions at $\sqrt{s} = 7$ TeV for $|\eta(D)| < 2.1$ in the high-p_{T} range, $20 < p_{\mathrm{T}}(D) < 100$ GeV, are measured to be

$$\begin{aligned}
\sigma^{\mathrm{vis}}(D^{*\pm}) &= 988 \pm 45\,(\mathrm{stat}) \pm 81\,(\mathrm{syst}) \pm 35\,(\mathrm{lum}) \pm 15\,(\mathrm{br})\,\mathrm{nb}\,,\\
\sigma^{\mathrm{vis}}(D^{\pm}) &= 888 \pm 53\,(\mathrm{stat}) \pm 73\,(\mathrm{syst}) \pm 31\,(\mathrm{lum}) \pm 18\,(\mathrm{br})\,\mathrm{nb}\,,\\
\sigma^{\mathrm{vis}}(D_s^{\pm}) &= 512 \pm 83\,(\mathrm{stat}) \pm 52\,(\mathrm{syst}) \pm 18\,(\mathrm{lum}) \pm 30\,(\mathrm{br})\,\mathrm{nb}\,.
\end{aligned}$$

The POWHEG+PYTHIA predictions are

$$\begin{aligned}
\sigma^{\mathrm{vis}}(D^{*\pm}) &= 600^{+269}_{-137}\,(\mathrm{scale})^{+15}_{-21}\,(m_Q)^{+25}_{-34}\,(\mathrm{PDF}\oplus\alpha_s)^{+126}_{-111}\,(\mathrm{hadr})\,\mathrm{nb}\,,\\
\sigma^{\mathrm{vis}}(D^{\pm}) &= 480^{+208}_{-109}\,(\mathrm{scale})^{+6}_{-11}\,(m_Q)^{+20}_{-27}\,(\mathrm{PDF}\oplus\alpha_s)^{+121}_{-71}\,(\mathrm{hadr})\,\mathrm{nb}\,,\\
\sigma^{\mathrm{vis}}(D_s^{\pm}) &= 225^{+106}_{-47}\,(\mathrm{scale})\ ^{+9}_{-8}\,(m_Q)^{+9}_{-13}\,(\mathrm{PDF}\oplus\alpha_s)\ ^{+40}_{-49}\,(\mathrm{hadr})\,\mathrm{nb}\,.
\end{aligned}$$

	$\sigma^{\text{vis}}(D^{*\pm})$		$\sigma^{\text{vis}}(D^{\pm})$		$\sigma^{\text{vis}}(D_s^{\pm})$	
Range	low-p_{T}	high-p_{T}	low-p_{T}	high-p_{T}	low-p_{T}	high-p_{T}
[units]	[μb]	[nb]	[μb]	[nb]	[μb]	[nb]
ATLAS	331 ± 36	988 ± 100	328 ± 34	888 ± 97	160 ± 37	512 ± 104
GM-VFNS	340^{+130}_{-150}	1000^{+120}_{-150}	350^{+150}_{-160}	980^{+120}_{-150}	147^{+54}_{-66}	470^{+56}_{-69}
FONLL	202^{+125}_{-79}	753^{+123}_{-104}	174^{+105}_{-66}	617^{+103}_{-86}	-	-
POWHEG+PYTHIA	158^{+179}_{-85}	600^{+300}_{-180}	134^{+148}_{-70}	480^{+240}_{-130}	62^{+64}_{-31}	225^{+114}_{-69}
POWHEG+HERWIG	137^{+147}_{-72}	690^{+380}_{-160}	121^{+129}_{-64}	580^{+280}_{-140}	51^{+50}_{-25}	268^{+107}_{-62}
MC@NLO	157^{+125}_{-72}	980^{+460}_{-290}	140^{+112}_{-65}	810^{+390}_{-260}	58^{+42}_{-25}	345^{+175}_{-87}

Table 3: The visible low-p_{T}, $3.5 < p_{\text{T}}(D) < 20$ GeV, and high-p_{T}, $20 < p_{\text{T}}(D) < 100$ GeV, cross sections of $D^{*\pm}$, $D^{\pm}$ and $D_s^{\pm}$ production with $|\eta| < 2.1$. The measurements are compared with the GM-VFNS [20–22], FONLL [17–19, 23], POWHEG+PYTHIA [11, 27], POWHEG+HERWIG [27, 28] and MC@NLO [26, 28] predictions. The data uncertainties are the total uncertainties obtained as sums in quadrature of the statistical, systematic, luminosity and branching-fraction uncertainties. The prediction uncertainties are the total uncertainties obtained as sums in quadrature of all considered sources of the theoretical uncertainty (see text).

p_{T} range	$\text{d}\sigma/\text{d}p_{\text{T}}(D^{*\pm})$ [μb/GeV]	$\text{d}\sigma/\text{d}p_{\text{T}}(D^{\pm})$ [μb/GeV]
3.5 – 5.0	145 ± 15 ± 14	127 ± 13 ± 12
5.0 – 6.5	43.4 ± 4.2 ± 3.6	51.9 ± 4.3 ± 4.2
6.5 – 8.0	20.8 ± 1.9 ± 1.7	20.0 ± 2.3 ± 1.6
8 – 12	6.34 ± 0.50 ± 0.51	6.29 ± 0.56 ± 0.51
12 – 20	$(757 \pm 101 \pm 65) \times 10^{-3}$	$(583 \pm 88 \pm 50) \times 10^{-3}$
20 – 30	$(78.8 \pm 5.6 \pm 6.4) \times 10^{-3}$	$(73.6 \pm 5.5 \pm 5.9) \times 10^{-3}$
30 – 40	$(13.3 \pm 1.2 \pm 1.2) \times 10^{-3}$	$(11.9 \pm 1.2 \pm 1.0) \times 10^{-3}$
40 – 60	$(2.52 \pm 0.21 \pm 0.20) \times 10^{-3}$	$(2.05 \pm 0.18 \pm 0.16) \times 10^{-3}$
60 – 100	$(131 \pm 31 \pm 11) \times 10^{-6}$	$(175 \pm 41 \pm 15) \times 10^{-6}$

Table 4: The measured differential cross sections $\text{d}\sigma/\text{d}p_{\text{T}}$ of $D^{*\pm}$ and $D^{\pm}$ production with $|\eta| < 2.1$. The first and second errors are the statistical and systematic uncertainties, respectively. The systematic uncertainties corresponding to the tracking (δ_2) uncertainties (Table 2) are strongly correlated. The fully correlated uncertainties linked with the luminosity measurement (3.5%) and branching fractions (1.5% and 2.1% for $D^{*\pm}$ and $D^{\pm}$, respectively) are not shown.

The FONLL predictions for D^{*+} and D^{+} are

$$\sigma^{\text{vis}}(D^{*\pm}) = 753^{+116}_{-98}\,(\text{scale})^{+28}_{-18}\,(m_Q) \pm 41\,(\text{PDF}) \pm 17\,(\text{ff})\,\mu\text{b}\,,$$

$$\sigma^{\text{vis}}(D^{\pm}) = 617\ ^{+92}_{-78}\,(\text{scale})^{+37}_{-21}\,(m_Q) \pm 33\,(\text{PDF}) \pm 23\,(\text{ff})\,\mu\text{b}\,.$$

$\|\eta\|$ range	$d\sigma/d\|\eta\|(D^{*\pm})$ [μb]	$d\sigma/d\|\eta\|(D^{\pm})$ [μb]
0.0 – 0.2	176 ± 21 ± 14	165 ± 20 ± 13
0.2 – 0.5	158 ± 17 ± 12	164 ± 16 ± 13
0.5 – 0.8	149 ± 15 ± 12	165 ± 15 ± 13
0.8 – 1.3	156 ± 14 ± 14	157 ± 17 ± 13
1.3 – 2.1	171 ± 23 ± 19	142 ± 19 ± 18

Table 5: The measured differential cross sections $d\sigma/d|\eta|$ of $D^{*\pm}$ and $D^{\pm}$ production with $3.5 < p_T < 20$ GeV. The first and second errors are the statistical and systematic uncertainties, respectively. The systematic uncertainty fractions corresponding to the tracking (δ_2) uncertainties (Table 2) are strongly correlated. The fully correlated uncertainties linked with the luminosity measurement (3.5%) and branching fractions (1.5% and 2.1% for $D^{*\pm}$ and $D^{\pm}$, respectively) are not shown.

$\|\eta\|$ range	$d\sigma/d\|\eta\|(D^{*\pm})$ [nb]	$d\sigma/d\|\eta\|(D^{\pm})$ [nb]
0.0 – 0.2	591 ± 66 ± 46	579 ± 80 ± 46
0.2 – 0.5	584 ± 54 ± 46	543 ± 51 ± 42
0.5 – 0.8	638 ± 55 ± 49	510 ± 51 ± 42
0.8 – 1.3	446 ± 43 ± 35	408 ± 46 ± 33
1.3 – 2.1	358 ± 49 ± 40	350 ± 65 ± 39

Table 6: The measured differential cross sections $d\sigma/d|\eta|$ of $D^{*\pm}$ and $D^{\pm}$ production with $20 < p_T < 100$ GeV. The first and second errors are the statistical and systematic uncertainties, respectively. The systematic uncertainty fractions corresponding to the tracking (δ_2) uncertainties (Table 2) are strongly correlated. The fully correlated uncertainties linked with the luminosity measurement (3.5%) and branching fractions (1.5% and 2.1% for $D^{*\pm}$ and $D^{\pm}$, respectively) are not shown.

The visible low-p_T and high-p_T $D^{*\pm}$, $D^{\pm}$ and $D_s^{\pm}$ production cross sections are compared in Table 3 with the NLO QCD predictions. The FONLL, MC@NLO and POWHEG predictions are consistent with the data within the large theoretical uncertainties, with the central values of the predictions lying below the measurements. The GM-VFNS predictions agree with data.

The differential cross sections $d\sigma/dp_T$ and $d\sigma/d|\eta|$ for $D^{*\pm}$ and $D^{\pm}$ production are shown in Tables 4-6 and compared in Figs. 4-6 with the NLO QCD predictions. The FONLL, MC@NLO and POWHEG predictions are generally below the data. They are consistent with the data in the measured $p_T(D)$ and $|\eta(D)|$ ranges within the large theoretical uncertainties. The FONLL and POWHEG predictions reproduce shapes of the data distributions. The p_T shape of the MC@NLO prediction is harder than that for the data. The $|\eta|$ shape of the MC@NLO prediction in the high-p_T range differs from the data and all other predictions. The GM-VFNS predictions agree with data in both shape and normalisation.

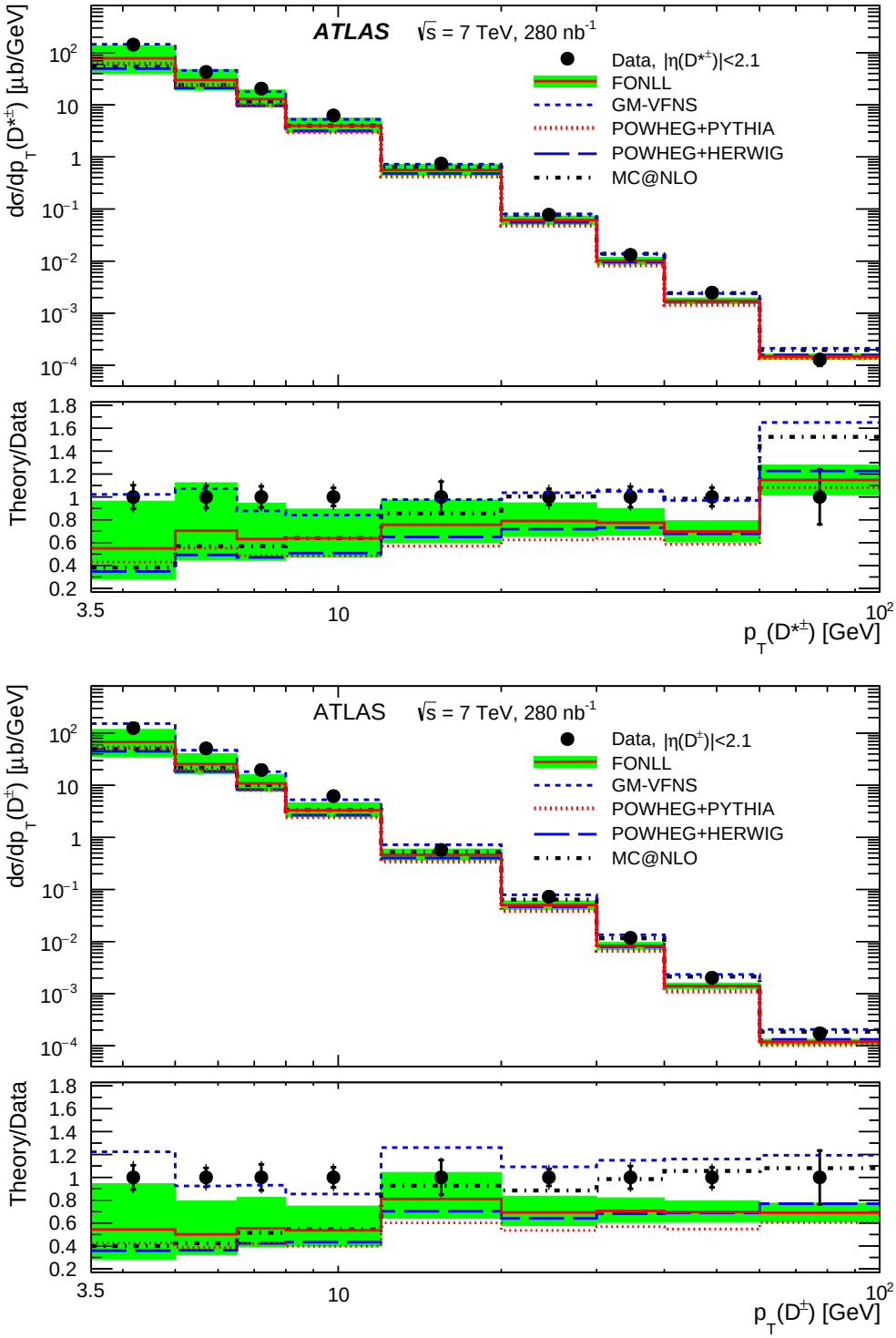

Figure 4: Differential cross sections for $D^{*\pm}$ (top) and $D^{\pm}$ (bottom) mesons as a function of p_{T} for data (points) compared to the NLO QCD calculations of FONLL, POWHEG+PYTHIA, POWHEG+HERWIG, MC@NLO and GM-VFNS (histograms). The data points are drawn in the bin centres. The inner error bars show the statistical uncertainties and the outer error bars show the statistical and systematic uncertainties added in quadrature. Uncertainties linked with the luminosity measurement (3.5%) and branching fractions (1.5% and 2.1% for $D^{*\pm}$ and $D^{\pm}$, respectively) are not included in the shown systematic uncertainties. The bands show the estimated theoretical uncertainty of the FONLL calculation.

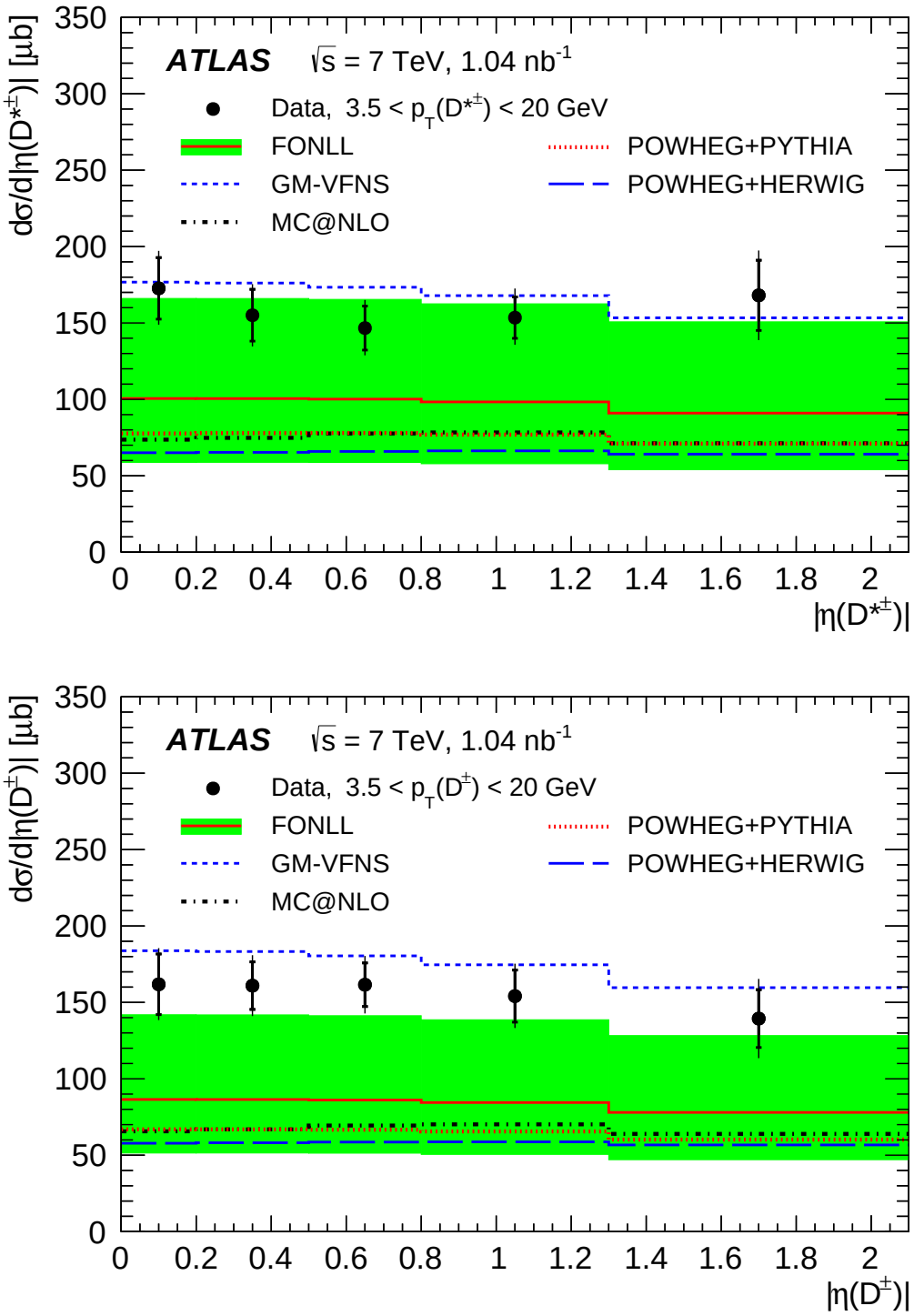

Figure 5: Differential cross sections for $D^{*\pm}$ (top) and $D^{\pm}$ (bottom) mesons with $3.5 < p_{\mathrm{T}}(D) < 20$ GeV as a function of $|\eta|$ for data (points) compared to the NLO QCD calculations of FONLL, POWHEG+PYTHIA, POWHEG+HERWIG, MC@NLO and GM-VFNS (histograms). The data points are drawn in the bin centres. The inner error bars show the statistical uncertainties and the outer error bars show the statistical and systematic uncertainties added in quadrature. Uncertainties linked with the luminosity measurement (3.5%) and branching fractions (1.5% and 2.1% for $D^{*\pm}$ and $D^{\pm}$, respectively) are not included in the shown systematic uncertainties. The bands show the estimated theoretical uncertainty of the FONLL calculation.

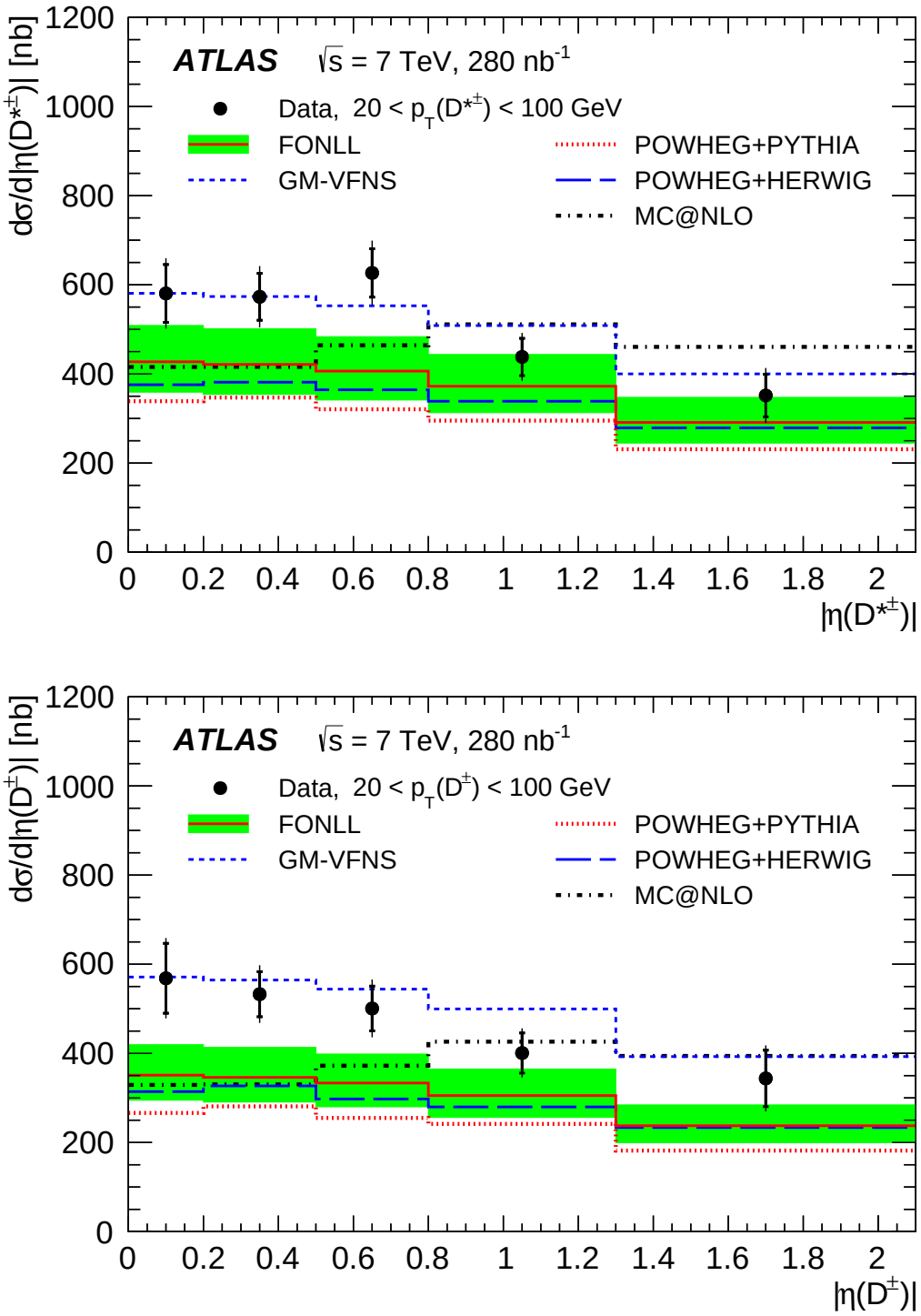

Figure 6: Differential cross sections for $D^{*\pm}$ (top) and $D^{\pm}$ (bottom) mesons with $20 < p_{\mathrm{T}}(D) < 100$ GeV as a function of $|\eta|$ for data (points) compared to the NLO QCD calculations of FONLL, POWHEG+PYTHIA, POWHEG+HERWIG, MC@NLO and GM-VFNS (histograms). The data points are drawn in the bin centres. The inner error bars show the statistical uncertainties and the outer error bars show the statistical and systematic uncertainties added in quadrature. Uncertainties linked with the luminosity measurement (3.5%) and branching fractions (1.5% and 2.1% for $D^{*\pm}$ and $D^{\pm}$, respectively) are not included in the shown systematic uncertainties. The bands show the estimated theoretical uncertainty of the FONLL calculation.

9 Extrapolation to the full kinematic phase space

The visible kinematic range covers only a small fraction of produced charmed mesons. To get some insight into the general properties of charm production and hadronisation at the LHC, the visible low-p_{T} D cross sections are extrapolated to the cross sections in the full kinematic phase space after subtracting the cross-section fractions originating from beauty production. Assuming the validity of the QCD NLO calculations and QCD factorisation in the whole phase space, the extrapolation factors are calculated as ratios of the total NLO cross sections of D mesons produced in charm hadronisation, $\sigma^{\mathrm{tot}}_{c\bar{c}}(D)$, to those in the visible kinematic range. The extrapolation factors from the visible low-p_{T} D^{*+}, D^+ and D_s^+ cross sections to the full kinematic phase space are of the order 12–14.

The extrapolated D cross sections are used to calculate the total cross section of charm production in pp collisions at $\sqrt{s} = 7\,\mathrm{TeV}$, and two charm fragmentation ratios: the strangeness-suppression factor in charm fragmentation and the fraction of charged non-strange D mesons produced in a vector state. The GM-VFNS calculations cannot be used for extrapolation because they originate from the massless scheme. For estimation of the total cross section of charm production, the extrapolation is performed with the FONLL calculations. However, as the FONLL calculations are not available for D_s^+ production and do not include such a sophisticated fragmentation scheme as PYTHIA, the extrapolation for extraction of the charm fragmentation ratios is performed with the POWHEG+PYTHIA calculations.

The results obtained by extrapolating the visible high-p_{T} D cross sections agree with the results presented, but have larger extrapolation uncertainties.

9.1 Total charm production cross section

To calculate the total cross section of charm production, the total production cross section of a given D meson should be divided by twice the value of the corresponding charm fragmentation fraction from Table 1. The weighted mean of the two values calculated from $D^{*\pm}$ and $D^{\pm}$ cross sections is

$$\sigma^{\mathrm{tot}}_{c\bar{c}} = 8.6 \pm 0.3\,(\mathrm{stat}) \pm 0.7\,(\mathrm{syst}) \pm 0.3\,(\mathrm{lum}) \pm 0.2\,(\mathrm{ff})^{+3.8}_{-3.4}\,(\mathrm{extr})\,\mathrm{mb} \quad (\mathrm{ATLAS})\,,$$

where the fourth uncertainty is due to the uncertainty of the fragmentation fractions and the last uncertainty is due to the extrapolation procedure. The extrapolation uncertainty is determined by adding in quadrature the changes in results originating from all sources of the FONLL theoretical uncertainty (Section 4). The uncertainties in the charmed meson decay branching fractions, which are common to the measured cross sections and fragmentation fractions, do not affect the calculation of the total cross section of charm production.

The calculated total cross section of charm production can be compared with a similar calculation performed by the ALICE experiment [50]:

$$\sigma^{\mathrm{tot}}_{c\bar{c}} = 8.5 \pm 0.5\,(\mathrm{stat})^{+1.0}_{-2.4}\,(\mathrm{syst}) \pm 0.3\,(\mathrm{lum}) \pm 0.2\,(\mathrm{ff})^{+5.0}_{-0.4}(\mathrm{extr})\,\mathrm{mb} \quad (\mathrm{ALICE})\,.$$

The ATLAS and ALICE estimates of the total charm production cross section at LHC are in good agreement. Both estimations are performed using extrapolations outside the visible kinematic ranges with analogous FONLL calculations. The different extrapolation uncertainties of the two estimations are due to different visible kinematic ranges. ATLAS extrapolates from the kinematic range $3.5 < p_{\mathrm{T}}(D) < 20$ GeV and $|\eta(D)| < 2.1$, while the ALICE visible kinematic range is $1 < p_{\mathrm{T}}(D) < 24$ GeV and $|y(D)| < 0.5$.

9.2 Charm fragmentation ratios

The total cross sections for D production are used to calculate two fragmentation ratios for charged charmed mesons: the strangeness-suppression factor, $\gamma_{s/d}$, and the fraction of charged non-strange D mesons produced in a vector state, P_{v}^{d}. The strangeness-suppression factor is calculated as the ratio of the $\sigma_{c\bar{c}}^{\mathrm{tot}}(D_s^+)$ to the sum of $\sigma_{c\bar{c}}^{\mathrm{tot}}(D^{*+})$ and that part of $\sigma_{c\bar{c}}^{\mathrm{tot}}(D^+)$ which does not originate from D^{*+} decays:

$$\gamma_{s/d} = \frac{\sigma_{c\bar{c}}^{\mathrm{tot}}(D_s^+)}{\sigma_{c\bar{c}}^{\mathrm{tot}}(D^{*+}) + \sigma_{c\bar{c}}^{\mathrm{tot}}(D^+) - \sigma_{c\bar{c}}^{\mathrm{tot}}(D^{*+}) \cdot (1 - \mathcal{B}_{D^{*+}\to D^0\pi^+})} = \frac{\sigma_{c\bar{c}}^{\mathrm{tot}}(D_s^+)}{\sigma_{c\bar{c}}^{\mathrm{tot}}(D^+) + \sigma_{c\bar{c}}^{\mathrm{tot}}(D^{*+}) \cdot \mathcal{B}_{D^{*+}\to D^0\pi^+}},$$

where $\mathcal{B}_{D^{*+}\to D^0\pi^+} = 0.677 \pm 0.005$ [47] is the branching fraction of the $D^{*+} \to D^0\pi^+$ decay. The fraction of charged non-strange D mesons produced in a vector state is calculated as the ratio of $\sigma_{c\bar{c}}^{\mathrm{tot}}(D^{*+})$ to the sum of $\sigma_{c\bar{c}}^{\mathrm{tot}}(D^{*+})$ and that part of $\sigma_{c\bar{c}}^{\mathrm{tot}}(D^+)$ which does not originate from D^{*+} decays:

$$P_{\mathrm{v}}^{d} = \frac{\sigma_{c\bar{c}}^{\mathrm{tot}}(D^{*+})}{\sigma_{c\bar{c}}^{\mathrm{tot}}(D^{*+}) + \sigma_{c\bar{c}}^{\mathrm{tot}}(D^+) - \sigma_{c\bar{c}}^{\mathrm{tot}}(D^{*+}) \cdot (1 - \mathcal{B}_{D^{*+}\to D^0\pi^+})} = \frac{\sigma_{c\bar{c}}^{\mathrm{tot}}(D^{*+})}{\sigma_{c\bar{c}}^{\mathrm{tot}}(D^+) + \sigma_{c\bar{c}}^{\mathrm{tot}}(D^{*+}) \cdot \mathcal{B}_{D^{*+}\to D^0\pi^+}}.$$

The large extrapolation uncertainties, which affect the extrapolated cross sections, are expected to nearly cancel out in the ratios. However, the calculations of the ratios are affected by details of the fragmentation simulation. To determine the extrapolation uncertainties, the following variations of the PYTHIA fragmentation, in addition to the POWHEG+PYTHIA theoretical uncertainty (Section 4), are considered:

- the Bowler fragmentation function parameter r_c is varied from the predicted value of 1 to 0.5; the a and b parameters of the Lund symmetric function are varied by ±20% around their default values;
- the PYTHIA parameter for the strangeness suppression is taken to be 0.3 ± 0.1;
- the PYTHIA parameter for the fraction of the lowest-mass charmed mesons produced in a vector state is taken to be 0.6 ± 0.1;
- the PYTHIA parameters for production rates of the excited charmed and charmed-strange mesons are varied by ±50% around the central values tuned to reproduce the measured fractions of c quarks hadronising into D_1^0, D_2^{*0} or D_{s1}^+ [51].

Using the extrapolated cross sections, the strangeness-suppression factor and the fraction P_{v}^{d} are

$$\gamma_{s/d} = 0.26 \pm 0.05\,(\mathrm{stat}) \pm 0.02\,(\mathrm{syst}) \pm 0.02\,(\mathrm{br}) \pm 0.01\,(\mathrm{extr}),$$

$$P_{\mathrm{v}}^{d} = 0.56 \pm 0.03\,(\mathrm{stat}) \pm 0.01\,(\mathrm{syst}) \pm 0.01\,(\mathrm{br}) \pm 0.02\,(\mathrm{extr}).$$

The measured P_{v}^{d} fraction is smaller than the naive spin-counting prediction of 0.75, suggesting the charm-quark mass is not large enough to ensure a precise description of charm fragmentation by heavy-quark effective theory [52]. The predictions of the thermodynamical approach [53] and the string fragmentation approach [54], which both predict 2/3 for the fraction, are closer to, but still above, the measured value.

The measured charm fragmentation ratios agree with those measured by ALICE [5,6] and those measured at the HERA collider in $e^{\pm}p$ collisions [55–58]. They can also be compared with results obtained in e^+e^- annihilations at LEP. The LEP fragmentation ratios are calculated using the fragmentation fractions from Table 1:

$$\gamma_{s/d}^{\mathrm{LEP}} = \frac{f(c \to D_s^+)}{f(c \to D^+) + f(c \to D^{*+}) \cdot \mathcal{B}_{D^{*+}\to D^0\pi^+}} = 0.24 \pm 0.02 \pm 0.01\,(\mathrm{br}),$$

$$P_{\mathrm{v}}^{\mathrm{LEP}} = \frac{f(c \to D^{*+})}{f(c \to D^{+}) + f(c \to D^{*+}) \cdot \mathcal{B}_{D^{*+} \to D^{0}\pi^{+}}} = 0.61 \pm 0.02 \pm 0.01\,(\mathrm{br})\,,$$

where the first uncertainties are the combined statistical and systematic uncertainties of the LEP measurements and the second uncertainties originate from uncertainties of the relevant branching fractions. The measurements agree within experimental uncertainties, in agreement with the hypothesis of charm fragmentation universality.

10 Summary

The production of $D^{*\pm}$, $D^{\pm}$ and $D_s^{\pm}$ charmed mesons has been measured in the kinematic region $3.5 < p_{\mathrm{T}}(D) < 100$ GeV and $|\eta(D)| < 2.1$ with the ATLAS detector in pp collisions at $\sqrt{s} = 7$ TeV at the LHC, using an integrated luminosity of up to $280\,\mathrm{nb}^{-1}$. The differential cross sections $\mathrm{d}\sigma/\mathrm{d}p_{\mathrm{T}}$ and $\mathrm{d}\sigma/\mathrm{d}|\eta|$ for $D^{*\pm}$ and $D^{\pm}$ production have been determined and compared with a number of NLO QCD predictions. The FONLL [17–19, 23], MC@NLO [24, 26] and POWHEG [25, 27] predictions are generally below the data. They are consistent with the data in normalisation within the large theoretical uncertainties. The FONLL and POWHEG predictions reproduce the shapes of the data distributions while the MC@NLO predictions show deviations from the shapes in the data. The GM-VFNS [20–22] predictions agree with data in both shape and normalisation.

Using the visible D cross sections and an extrapolation to the full kinematic phase space, the strangeness-suppression factor in charm fragmentation, the fraction of charged non-strange D mesons produced in a vector state, and the total cross section of charm production in pp collisions at $\sqrt{s} = 7$ TeV have been calculated. The fragmentation ratios agree with those obtained by the ALICE collaboration at the LHC, and those measured in e^+e^- annihilations at LEP and in $e^{\pm}p$ collisions at HERA. The total cross section of charm production at $\sqrt{s} = 7$ TeV agree with the result of the ALICE collaboration.

Acknowledgements

We thank CERN for the very successful operation of the LHC, as well as the support staff from our institutions without whom ATLAS could not be operated efficiently.

We acknowledge the support of ANPCyT, Argentina; YerPhI, Armenia; ARC, Australia; BMWFW and FWF, Austria; ANAS, Azerbaijan; SSTC, Belarus; CNPq and FAPESP, Brazil; NSERC, NRC and CFI, Canada; CERN; CONICYT, Chile; CAS, MOST and NSFC, China; COLCIENCIAS, Colombia; MSMT CR, MPO CR and VSC CR, Czech Republic; DNRF, DNSRC and Lundbeck Foundation, Denmark; IN2P3-CNRS, CEA-DSM/IRFU, France; GNSF, Georgia; BMBF, HGF, and MPG, Germany; GSRT, Greece; RGC, Hong Kong SAR, China; ISF, I-CORE and Benoziyo Center, Israel; INFN, Italy; MEXT and JSPS, Japan; CNRST, Morocco; FOM and NWO, Netherlands; RCN, Norway; MNiSW and NCN, Poland; FCT, Portugal; MNE/IFA, Romania; MES of Russia and NRC KI, Russian Federation; JINR; MESTD, Serbia; MSSR, Slovakia; ARRS and MIZŠ, Slovenia; DST/NRF, South Africa; MINECO, Spain; SRC and Wallenberg Foundation, Sweden; SERI, SNSF and Cantons of Bern and Geneva, Switzerland; MOST, Taiwan; TAEK, Turkey; STFC, United Kingdom; DOE and NSF, United States of America. In addition, individual groups and members have received support from BCKDF, the Canada Council, CANARIE, CRC, Compute Canada, FQRNT, and the Ontario Innovation Trust, Canada;

EPLANET, ERC, FP7, Horizon 2020 and Marie Skłodowska-Curie Actions, European Union; Investissements d'Avenir Labex and Idex, ANR, Region Auvergne and Fondation Partager le Savoir, France; DFG and AvH Foundation, Germany; Herakleitos, Thales and Aristeia programmes co-financed by EU-ESF and the Greek NSRF; BSF, GIF and Minerva, Israel; BRF, Norway; the Royal Society and Leverhulme Trust, United Kingdom.

The crucial computing support from all WLCG partners is acknowledged gratefully, in particular from CERN and the ATLAS Tier-1 facilities at TRIUMF (Canada), NDGF (Denmark, Norway, Sweden), CC-IN2P3 (France), KIT/GridKA (Germany), INFN-CNAF (Italy), NL-T1 (Netherlands), PIC (Spain), ASGC (Taiwan), RAL (UK) and BNL (USA) and in the Tier-2 facilities worldwide.

References

[1] ATLAS Collaboration, JINST 3 (2008) S08003.

[2] ATLAS Collaboration, Phys. Rev. D 85 (2012) 052005, arXiv:1112.4432 [hep-ex].

[3] ATLAS Collaboration, Nucl. Phys. B 864 (2012) 341, arXiv:1206.3122 [hep-ex].

[4] ATLAS Collaboration, JHEP 05 (2014) 068, arXiv:1402.6263 [hep-ex].

[5] ALICE Collaboration, B. Abelev et al., JHEP 01 (2012) 128, arXiv:1111.1553 [hep-ex].

[6] ALICE Collaboration, B. Abelev et al., Phys. Lett. B 718 (2012) 279, arXiv:1208.1948 [hep-ex].

[7] LHCb Collaboration, R. Aaij et al., Nucl. Phys. B 871 (2013) 1, arXiv:1302.2864 [hep-ex].

[8] CDF Collaboration, D. Acosta et al., Phys. Rev. Lett. 91 (2003) 241804, arXiv:hep-ex/0307080.

[9] ATLAS Collaboration, Eur. Phys. J. C 72 (2012) 1849, arXiv:1110.1530 [hep-ex].

[10] ATLAS Collaboration, Eur. Phys. J. C 73 (2013) 2518, arXiv:1302.4393 [hep-ex].

[11] T. Sjöstrand, S. Mrenna, P. Skands, JHEP 05 (2006) 026.

[12] A. Sherstnev and R. S. Thorne, Eur. Phys. J. C 55 (2008) 553, arXiv:0711.2473 [hep-ph].

[13] ATLAS Collaboration, New J. Phys. 13 (2011) 053033, arXiv:1012.5104 [hep-ex].

[14] ATLAS Collaboration, Eur. Phys. J. C 70 (2010) 823, arXiv:1005.4568 [hep-ex].

[15] S. Agostinelli et al., Nucl. Instr. Meth. A 506 (2003) 250.

[16] J. Allison et al., IEEE Trans. Nucl. Sci. 53 (2006) 270.

[17] M. Cacciari, M. Greco and P. Nason, JHEP 05 (1998) 007, arXiv:hep-ph/9803400.

[18] M. Cacciari, P. Nason, JHEP 09 (2003) 006, arXiv:hep-ph/0306212.

[19] M. Cacciari et al., JHEP 07 (2004) 033, arXiv:hep-ph/0312132.

[20] B. A. Kniehl, G. Kramer, I. Schienbein and H. Spiesberger, Phys. Rev. D 71 (2005) 014018, arXiv:hep-ph/0410289.

[21] B. A. Kniehl, G. Kramer, I. Schienbein and H. Spiesberger, Phys. Rev. Lett. 96 (2006) 012001, arXiv:hep-ph/0508129.

[22] B. A. Kniehl, G. Kramer, I. Schienbein and H. Spiesberger, Phys. Rev. D 79 (2009) 094009, arXiv:0901.4130 [hep-ph].

[23] M. Cacciari et al., JHEP 10 (2012) 137, arXiv:1012.5104 [hep-ph], http://www.lpthe.jussieu.fr/~cacciari/fonll/fonllform.html.

[24] S. Frixione and B. R. Webber, JHEP 06 (2002) 029, arXiv:hep-ph/0204244.

[25] P. Nason, JHEP 11 (2004) 040, arXiv:hep-ph/0409146.

[26] S. Frixione, P. Nason and B. R. Webber, JHEP 08 (2003) 007, arXiv:hep-ph/0305252. An extended version of the MC@NLO code for $c\bar{c}$ production calculations has been provided by the authors.

[27] S. Frixione, P. Nason and G. Ridolfi, JHEP 09 (2007) 126, arXiv:0707.3088 [hep-ph].

[28] G. Corcella et al., JHEP 01 (2001) 010, arXiv:hep-ph/0011363.

[29] T. Kneesch, B. A. Kniehl, G. Kramer and I. Schienbein, Nucl. Phys. B 799 (2008) 34, arXiv:0712.0481 [hep-ph].

[30] P. M. Nadolsky et al., Phys. Rev. D 78 (2008) 013004, arXiv:0802.0007 [hep-ph].

[31] M. Cacciari, P. Nason and C. Oleari, JHEP 04 (2006) 006, arXiv:hep-ph/0510032.

[32] B. R. Webber, Nucl. Phys. B 238 (1984) 492.

[33] B. Andersson et al., Phys. Rep. 97 (1983) 31.

[34] M. G. Bowler, Z. Phys. C 11 (1981) 169.

[35] B. Andersson, G. Gustafson, B. Söderberg, Z. Phys. C 20 (1983) 317.

[36] L. Gladilin, Eur. Phys. J. C 75 (2015) 19, arXiv:1404.3888 [hep-ex].

[37] M. Botje et al., 2011, arXiv:1101.0538 [hep-ph].

[38] C. Peterson et al., Phys. Rev. D 27 (1983) 105.

[39] J. Chrin, Z. Phys. C 36 (1987) 163.

[40] M. Cacciari and M. Greco, Phys. Rev. D 55 (1997) 7134, arXiv:hep-ph/9702389.

[41] P. Nason and C. Oleari, Phys. Lett. B 447 (1999) 327, arXiv:hep-ph/9811206.

[42] OPAL Collaboration, G. Abbiendi et al., Eur. Phys. J. C 29 (2003) 463, arXiv:hep-ex/0210031.

[43] ZEUS Collaboration, S. Chekanov et al., JHEP 04 (2009) 082, arXiv:0901.1210 [hep-ex].

[44] ATLAS Collaboration, Eur. Phys. J. C 70 (2010) 787, arXiv:1004.5293 [hep-ex].

[45] ATLAS Collaboration, ATLAS-CONF-2010-069 (2010), http://cds.cern.ch/record/1281344.

[46] ATLAS Collaboration, JHEP 09 (2010) 056, arXiv:1005.5254 [hep-ex].

[47] K. A. Olive et al. (Particle Data Group), Chin. Phys. C 38 (2014) 090001.

[48] ZEUS Collaboration, S. Chekanov et al., Eur. Phys. J. C 44 (2005) 13, arXiv:hep-ex/0505008.

[49] CLEO Collaboration, J. P. Alexander et al, Phys. Rev. Lett. 100 (2008) 161804, arXiv:0801.0680 [hep-ex].

[50] ALICE Collaboration, B. Abelev et al., JHEP 07 (2012) 191, arXiv:1205.4007 [hep-ex].

[51] ZEUS Collaboration, S. Chekanov et al., Eur. Phys. J. C 60 (2009) 25, arXiv:0807.1290 [hep-ex].

[52] A. David, Phys. Let. B 644 (2007) 224.

[53] F. Becattini, Z. Phys. C 69 (1996) 485.

[54] Y. Pei, Z. Phys. C 72 (1996) 39.

[55] H1 Collaboration, A. Aktas et al., Eur. Phys. J. C 38 (2005) 447, arXiv:hep-ex/0408149.

[56] ZEUS Collaboration, S. Chekanov et al., Eur. Phys. J. C 44 (2005) 351, arXiv:hep-ex/0508019.

[57] ZEUS Collaboration, S. Chekanov et al., JHEP 07 (2007) 074, arXiv:0704.3562 [hep-ex].

[58] ZEUS Collaboration, H. Abramowicz et al., JHEP 09 (2013) 058, arXiv:1306.4862 [hep-ex].

The ATLAS Collaboration

G. Aad[85], B. Abbott[113], J. Abdallah[151], O. Abdinov[11], R. Aben[107], M. Abolins[90], O.S. AbouZeid[158], H. Abramowicz[153], H. Abreu[152], R. Abreu[30], Y. Abulaiti[146a,146b], B.S. Acharya[164a,164b,a], L. Adamczyk[38a], D.L. Adams[25], J. Adelman[108], S. Adomeit[100], T. Adye[131], A.A. Affolder[74], T. Agatonovic-Jovin[13], J.A. Aguilar-Saavedra[126a,126f], S.P. Ahlen[22], F. Ahmadov[65,b], G. Aielli[133a,133b], H. Akerstedt[146a,146b], T.P.A. Åkesson[81], G. Akimoto[155], A.V. Akimov[96], G.L. Alberghi[20a,20b], J. Albert[169], S. Albrand[55], M.J. Alconada Verzini[71], M. Aleksa[30], I.N. Aleksandrov[65], C. Alexa[26a], G. Alexander[153], T. Alexopoulos[10], M. Alhroob[113], G. Alimonti[91a], L. Alio[85], J. Alison[31], S.P. Alkire[35], B.M.M. Allbrooke[18], P.P. Allport[18], A. Aloisio[104a,104b], A. Alonso[36], F. Alonso[71], C. Alpigiani[76], A. Altheimer[35], B. Alvarez Gonzalez[30], D. Álvarez Piqueras[167], M.G. Alviggi[104a,104b], B.T. Amadio[15], K. Amako[66], Y. Amaral Coutinho[24a], C. Amelung[23], D. Amidei[89], S.P. Amor Dos Santos[126a,126c], A. Amorim[126a,126b], S. Amoroso[48], N. Amram[153], G. Amundsen[23], C. Anastopoulos[139], L.S. Ancu[49], N. Andari[30], T. Andeen[35], C.F. Anders[58b], G. Anders[30], J.K. Anders[74], K.J. Anderson[31], A. Andreazza[91a,91b], V. Andrei[58a], S. Angelidakis[9], I. Angelozzi[107], P. Anger[44], A. Angerami[35], F. Anghinolfi[30], A.V. Anisenkov[109,c], N. Anjos[12], A. Annovi[124a,124b], M. Antonelli[47], A. Antonov[98], J. Antos[144b], F. Anulli[132a], M. Aoki[66], L. Aperio Bella[18], G. Arabidze[90], Y. Arai[66], J.P. Araque[126a], A.T.H. Arce[45], F.A. Arduh[71], J-F. Arguin[95], S. Argyropoulos[42], M. Arik[19a], A.J. Armbruster[30], O. Arnaez[30], V. Arnal[82], H. Arnold[48], M. Arratia[28], O. Arslan[21], A. Artamonov[97], G. Artoni[23], S. Asai[155], N. Asbah[42], A. Ashkenazi[153], B. Åsman[146a,146b], L. Asquith[149], K. Assamagan[25], R. Astalos[144a], M. Atkinson[165], N.B. Atlay[141], B. Auerbach[6], K. Augsten[128], M. Aurousseau[145b], G. Avolio[30], B. Axen[15], M.K. Ayoub[117], G. Azuelos[95,d], M.A. Baak[30], A.E. Baas[58a], C. Bacci[134a,134b], H. Bachacou[136], K. Bachas[154], M. Backes[30], M. Backhaus[30], P. Bagiacchi[132a,132b], P. Bagnaia[132a,132b], Y. Bai[33a], T. Bain[35], J.T. Baines[131], O.K. Baker[176], P. Balek[129], T. Balestri[148], F. Balli[84], E. Banas[39], Sw. Banerjee[173], A.A.E. Bannoura[175], H.S. Bansil[18], L. Barak[30], E.L. Barberio[88], D. Barberis[50a,50b], M. Barbero[85], T. Barillari[101], M. Barisonzi[164a,164b], T. Barklow[143], N. Barlow[28], S.L. Barnes[84], B.M. Barnett[131], R.M. Barnett[15], Z. Barnovska[5], A. Baroncelli[134a], G. Barone[49], A.J. Barr[120], F. Barreiro[82], J. Barreiro Guimarães da Costa[57], R. Bartoldus[143], A.E. Barton[72], P. Bartos[144a], A. Basalaev[123], A. Bassalat[117], A. Basye[165], R.L. Bates[53], S.J. Batista[158], J.R. Batley[28], M. Battaglia[137], M. Bauce[132a,132b], F. Bauer[136], H.S. Bawa[143,e], J.B. Beacham[111], M.D. Beattie[72], T. Beau[80], P.H. Beauchemin[161], R. Beccherle[124a,124b], P. Bechtle[21], H.P. Beck[17,f], K. Becker[120], M. Becker[83], S. Becker[100], M. Beckingham[170], C. Becot[117], A.J. Beddall[19b], A. Beddall[19b], V.A. Bednyakov[65], C.P. Bee[148], L.J. Beemster[107], T.A. Beermann[175], M. Begel[25], J.K. Behr[120], C. Belanger-Champagne[87], W.H. Bell[49], G. Bella[153], L. Bellagamba[20a], A. Bellerive[29], M. Bellomo[86], K. Belotskiy[98], O. Beltramello[30], O. Benary[153], D. Benchekroun[135a], M. Bender[100], K. Bendtz[146a,146b], N. Benekos[10], Y. Benhammou[153], E. Benhar Noccioli[49], J.A. Benitez Garcia[159b], D.P. Benjamin[45], J.R. Bensinger[23], S. Bentvelsen[107], L. Beresford[120], M. Beretta[47], D. Berge[107], E. Bergeaas Kuutmann[166], N. Berger[5], F. Berghaus[169], J. Beringer[15], C. Bernard[22], N.R. Bernard[86], C. Bernius[110], F.U. Bernlochner[21], T. Berry[77], P. Berta[129], C. Bertella[83], G. Bertoli[146a,146b], F. Bertolucci[124a,124b], C. Bertsche[113], D. Bertsche[113], M.I. Besana[91a], G.J. Besjes[106], O. Bessidskaia Bylund[146a,146b], M. Bessner[42], N. Besson[136], C. Betancourt[48], S. Bethke[101], A.J. Bevan[76], W. Bhimji[46], R.M. Bianchi[125], L. Bianchini[23], M. Bianco[30], O. Biebel[100], D. Biedermann[16], S.P. Bieniek[78], M. Biglietti[134a], J. Bilbao De Mendizabal[49], H. Bilokon[47], M. Bindi[54], S. Binet[117], A. Bingul[19b], C. Bini[132a,132b], C.W. Black[150], J.E. Black[143], K.M. Black[22], D. Blackburn[138], R.E. Blair[6], J.-B. Blanchard[136], J.E. Blanco[77], T. Blazek[144a], I. Bloch[42], C. Blocker[23], W. Blum[83,*], U. Blumenschein[54], G.J. Bobbink[107], V.S. Bobrovnikov[109,c], S.S. Bocchetta[81], A. Bocci[45], C. Bock[100], M. Boehler[48],

J.A. Bogaerts[30], D. Bogavac[13], A.G. Bogdanchikov[109], C. Bohm[146a], V. Boisvert[77], T. Bold[38a], V. Boldea[26a], A.S. Boldyrev[99], M. Bomben[80], M. Bona[76], M. Boonekamp[136], A. Borisov[130], G. Borissov[72], S. Borroni[42], J. Bortfeldt[100], V. Bortolotto[60a,60b,60c], K. Bos[107], D. Boscherini[20a], M. Bosman[12], J. Boudreau[125], J. Bouffard[2], E.V. Bouhova-Thacker[72], D. Boumediene[34], C. Bourdarios[117], N. Bousson[114], A. Boveia[30], J. Boyd[30], I.R. Boyko[65], I. Bozic[13], J. Bracinik[18], A. Brandt[8], G. Brandt[54], O. Brandt[58a], U. Bratzler[156], B. Brau[86], J.E. Brau[116], H.M. Braun[175,*], S.F. Brazzale[164a,164c], W.D. Breaden Madden[53], K. Brendlinger[122], A.J. Brennan[88], L. Brenner[107], R. Brenner[166], S. Bressler[172], K. Bristow[145c], T.M. Bristow[46], D. Britton[53], D. Britzger[42], F.M. Brochu[28], I. Brock[21], R. Brock[90], J. Bronner[101], G. Brooijmans[35], T. Brooks[77], W.K. Brooks[32b], J. Brosamer[15], E. Brost[116], J. Brown[55], P.A. Bruckman de Renstrom[39], D. Bruncko[144b], R. Bruneliere[48], A. Bruni[20a], G. Bruni[20a], M. Bruschi[20a], N. Bruscino[21], L. Bryngemark[81], T. Buanes[14], Q. Buat[142], P. Buchholz[141], A.G. Buckley[53], S.I. Buda[26a], I.A. Budagov[65], F. Buehrer[48], L. Bugge[119], M.K. Bugge[119], O. Bulekov[98], D. Bullock[8], H. Burckhart[30], S. Burdin[74], B. Burghgrave[108], S. Burke[131], I. Burmeister[43], E. Busato[34], D. Büscher[48], V. Büscher[83], P. Bussey[53], J.M. Butler[22], A.I. Butt[3], C.M. Buttar[53], J.M. Butterworth[78], P. Butti[107], W. Buttinger[25], A. Buzatu[53], A.R. Buzykaev[109,c], S. Cabrera Urbán[167], D. Caforio[128], V.M. Cairo[37a,37b], O. Cakir[4a], P. Calafiura[15], A. Calandri[136], G. Calderini[80], P. Calfayan[100], L.P. Caloba[24a], D. Calvet[34], S. Calvet[34], R. Camacho Toro[31], S. Camarda[42], P. Camarri[133a,133b], D. Cameron[119], L.M. Caminada[15], R. Caminal Armadans[165], S. Campana[30], M. Campanelli[78], A. Campoverde[148], V. Canale[104a,104b], A. Canepa[159a], M. Cano Bret[76], J. Cantero[82], R. Cantrill[126a], T. Cao[40], M.D.M. Capeans Garrido[30], I. Caprini[26a], M. Caprini[26a], M. Capua[37a,37b], R. Caputo[83], R. Cardarelli[133a], F. Cardillo[48], T. Carli[30], G. Carlino[104a], L. Carminati[91a,91b], S. Caron[106], E. Carquin[32a], G.D. Carrillo-Montoya[8], J.R. Carter[28], J. Carvalho[126a,126c], D. Casadei[78], M.P. Casado[12], M. Casolino[12], E. Castaneda-Miranda[145b], A. Castelli[107], V. Castillo Gimenez[167], N.F. Castro[126a,g], P. Catastini[57], A. Catinaccio[30], J.R. Catmore[119], A. Cattai[30], J. Caudron[83], V. Cavaliere[165], D. Cavalli[91a], M. Cavalli-Sforza[12], V. Cavasinni[124a,124b], F. Ceradini[134a,134b], B.C. Cerio[45], K. Cerny[129], A.S. Cerqueira[24b], A. Cerri[149], L. Cerrito[76], F. Cerutti[15], M. Cerv[30], A. Cervelli[17], S.A. Cetin[19c], A. Chafaq[135a], D. Chakraborty[108], I. Chalupkova[129], P. Chang[165], B. Chapleau[87], J.D. Chapman[28], D.G. Charlton[18], C.C. Chau[158], C.A. Chavez Barajas[149], S. Cheatham[152], A. Chegwidden[90], S. Chekanov[6], S.V. Chekulaev[159a], G.A. Chelkov[65,h], M.A. Chelstowska[89], C. Chen[64], H. Chen[25], K. Chen[148], L. Chen[33d,i], S. Chen[33c], X. Chen[33f], Y. Chen[67], H.C. Cheng[89], Y. Cheng[31], A. Cheplakov[65], E. Cheremushkina[130], R. Cherkaoui El Moursli[135e], V. Chernyatin[25,*], E. Cheu[7], L. Chevalier[136], V. Chiarella[47], J.T. Childers[6], G. Chiodini[73a], A.S. Chisholm[18], R.T. Chislett[78], A. Chitan[26a], M.V. Chizhov[65], K. Choi[61], S. Chouridou[9], B.K.B. Chow[100], V. Christodoulou[78], D. Chromek-Burckhart[30], J. Chudoba[127], A.J. Chuinard[87], J.J. Chwastowski[39], L. Chytka[115], G. Ciapetti[132a,132b], A.K. Ciftci[4a], D. Cinca[53], V. Cindro[75], I.A. Cioara[21], A. Ciocio[15], Z.H. Citron[172], M. Ciubancan[26a], A. Clark[49], B.L. Clark[57], P.J. Clark[46], R.N. Clarke[15], W. Cleland[125], C. Clement[146a,146b], Y. Coadou[85], M. Cobal[164a,164c], A. Coccaro[138], J. Cochran[64], L. Coffey[23], J.G. Cogan[143], B. Cole[35], S. Cole[108], A.P. Colijn[107], J. Collot[55], T. Colombo[58c], G. Compostella[101], P. Conde Muiño[126a,126b], E. Coniavitis[48], S.H. Connell[145b], I.A. Connelly[77], S.M. Consonni[91a,91b], V. Consorti[48], S. Constantinescu[26a], C. Conta[121a,121b], G. Conti[30], F. Conventi[104a,j], M. Cooke[15], B.D. Cooper[78], A.M. Cooper-Sarkar[120], T. Cornelissen[175], M. Corradi[132a,132b], F. Corriveau[87,k], A. Corso-Radu[163], A. Cortes-Gonzalez[12], G. Cortiana[101], G. Costa[91a], M.J. Costa[167], D. Costanzo[139], D. Côté[8], G. Cottin[28], G. Cowan[77], B.E. Cox[84], K. Cranmer[110], G. Cree[29], S. Crépé-Renaudin[55], F. Crescioli[80], W.A. Cribbs[146a,146b], M. Crispin Ortuzar[120], M. Cristinziani[21], V. Croft[106], G. Crosetti[37a,37b], T. Cuhadar Donszelmann[139], J. Cummings[176], M. Curatolo[47], C. Cuthbert[150], H. Czirr[141], P. Czodrowski[3], S. D'Auria[53], M. D'Onofrio[74], M.J. Da Cunha Sargedas De Sousa[126a,126b], C. Da Via[84], W. Dabrowski[38a],

A. Dafinca[120], T. Dai[89], O. Dale[14], F. Dallaire[95], C. Dallapiccola[86], M. Dam[36], J.R. Dandoy[31], N.P. Dang[48], A.C. Daniells[18], M. Danninger[168], M. Dano Hoffmann[136], V. Dao[48], G. Darbo[50a], S. Darmora[8], J. Dassoulas[3], A. Dattagupta[61], W. Davey[21], C. David[169], T. Davidek[129], E. Davies[120,l], M. Davies[153], P. Davison[78], Y. Davygora[58a], E. Dawe[88], I. Dawson[139], R.K. Daya-Ishmukhametova[86], K. De[8], R. de Asmundis[104a], S. De Castro[20a,20b], S. De Cecco[80], N. De Groot[106], P. de Jong[107], H. De la Torre[82], F. De Lorenzi[64], L. De Nooij[107], D. De Pedis[132a], A. De Salvo[132a], U. De Sanctis[149], A. De Santo[149], J.B. De Vivie De Regie[117], W.J. Dearnaley[72], R. Debbe[25], C. Debenedetti[137], D.V. Dedovich[65], I. Deigaard[107], J. Del Peso[82], T. Del Prete[124a,124b], D. Delgove[117], F. Deliot[136], C.M. Delitzsch[49], M. Deliyergiyev[75], A. Dell'Acqua[30], L. Dell'Asta[22], M. Dell'Orso[124a,124b], M. Della Pietra[104a,j], D. della Volpe[49], M. Delmastro[5], P.A. Delsart[55], C. Deluca[107], D.A. DeMarco[158], S. Demers[176], M. Demichev[65], A. Demilly[80], S.P. Denisov[130], D. Derendarz[39], J.E. Derkaoui[135d], F. Derue[80], P. Dervan[74], K. Desch[21], C. Deterre[42], P.O. Deviveiros[30], A. Dewhurst[131], S. Dhaliwal[23], A. Di Ciaccio[133a,133b], L. Di Ciaccio[5], A. Di Domenico[132a,132b], C. Di Donato[132a,132b], A. Di Girolamo[30], B. Di Girolamo[30], A. Di Mattia[152], B. Di Micco[134a,134b], R. Di Nardo[47], A. Di Simone[48], R. Di Sipio[158], D. Di Valentino[29], C. Diaconu[85], M. Diamond[158], F.A. Dias[46], M.A. Diaz[32a], E.B. Diehl[89], J. Dietrich[16], S. Diglio[85], A. Dimitrievska[13], J. Dingfelder[21], P. Dita[26a], S. Dita[26a], F. Dittus[30], F. Djama[85], T. Djobava[51b], J.I. Djuvsland[58a], M.A.B. do Vale[24c], D. Dobos[30], M. Dobre[26a], C. Doglioni[49], T. Dohmae[155], J. Dolejsi[129], Z. Dolezal[129], B.A. Dolgoshein[98,*], M. Donadelli[24d], S. Donati[124a,124b], P. Dondero[121a,121b], J. Donini[34], J. Dopke[131], A. Doria[104a], M.T. Dova[71], A.T. Doyle[53], E. Drechsler[54], M. Dris[10], E. Dubreuil[34], E. Duchovni[172], G. Duckeck[100], O.A. Ducu[26a,85], D. Duda[175], A. Dudarev[30], L. Duflot[117], L. Duguid[77], M. Dührssen[30], M. Dunford[58a], H. Duran Yildiz[4a], M. Düren[52], A. Durglishvili[51b], D. Duschinger[44], M. Dyndal[38a], C. Eckardt[42], K.M. Ecker[101], R.C. Edgar[89], W. Edson[2], N.C. Edwards[46], W. Ehrenfeld[21], T. Eifert[30], G. Eigen[14], K. Einsweiler[15], T. Ekelof[166], M. El Kacimi[135c], M. Ellert[166], S. Elles[5], F. Ellinghaus[83], A.A. Elliot[169], N. Ellis[30], J. Elmsheuser[100], M. Elsing[30], D. Emeliyanov[131], Y. Enari[155], O.C. Endner[83], M. Endo[118], J. Erdmann[43], A. Ereditato[17], G. Ernis[175], J. Ernst[2], M. Ernst[25], S. Errede[165], E. Ertel[83], M. Escalier[117], H. Esch[43], C. Escobar[125], B. Esposito[47], A.I. Etienvre[136], E. Etzion[153], H. Evans[61], A. Ezhilov[123], L. Fabbri[20a,20b], G. Facini[31], R.M. Fakhrutdinov[130], S. Falciano[132a], R.J. Falla[78], J. Faltova[129], Y. Fang[33a], M. Fanti[91a,91b], A. Farbin[8], A. Farilla[134a], T. Farooque[12], S. Farrell[15], S.M. Farrington[170], P. Farthouat[30], F. Fassi[135e], P. Fassnacht[30], D. Fassouliotis[9], M. Faucci Giannelli[77], A. Favareto[50a,50b], L. Fayard[117], P. Federic[144a], O.L. Fedin[123,m], W. Fedorko[168], S. Feigl[30], L. Feligioni[85], C. Feng[33d], E.J. Feng[6], H. Feng[89], A.B. Fenyuk[130], L. Feremenga[8], P. Fernandez Martinez[167], S. Fernandez Perez[30], J. Ferrando[53], A. Ferrari[166], P. Ferrari[107], R. Ferrari[121a], D.E. Ferreira de Lima[53], A. Ferrer[167], D. Ferrere[49], C. Ferretti[89], A. Ferretto Parodi[50a,50b], M. Fiascaris[31], F. Fiedler[83], A. Filipčič[75], M. Filipuzzi[42], F. Filthaut[106], M. Fincke-Keeler[169], K.D. Finelli[150], M.C.N. Fiolhais[126a,126c], L. Fiorini[167], A. Firan[40], A. Fischer[2], C. Fischer[12], J. Fischer[175], W.C. Fisher[90], E.A. Fitzgerald[23], I. Fleck[141], P. Fleischmann[89], S. Fleischmann[175], G.T. Fletcher[139], G. Fletcher[76], R.R.M. Fletcher[122], T. Flick[175], A. Floderus[81], L.R. Flores Castillo[60a], M.J. Flowerdew[101], A. Formica[136], A. Forti[84], D. Fournier[117], H. Fox[72], S. Fracchia[12], P. Francavilla[80], M. Franchini[20a,20b], D. Francis[30], L. Franconi[119], M. Franklin[57], M. Frate[163], M. Fraternali[121a,121b], D. Freeborn[78], S.T. French[28], F. Friedrich[44], D. Froidevaux[30], J.A. Frost[120], C. Fukunaga[156], E. Fullana Torregrosa[83], B.G. Fulsom[143], J. Fuster[167], C. Gabaldon[55], O. Gabizon[175], A. Gabrielli[20a,20b], A. Gabrielli[132a,132b], S. Gadatsch[107], S. Gadomski[49], G. Gagliardi[50a,50b], P. Gagnon[61], C. Galea[106], B. Galhardo[126a,126c], E.J. Gallas[120], B.J. Gallop[131], P. Gallus[128], G. Galster[36], K.K. Gan[111], J. Gao[33b,85], Y. Gao[46], Y.S. Gao[143,e], F.M. Garay Walls[46], F. Garberson[176], C. García[167], J.E. García Navarro[167], M. Garcia-Sciveres[15], R.W. Gardner[31], N. Garelli[143], V. Garonne[119], C. Gatti[47], A. Gaudiello[50a,50b], G. Gaudio[121a], B. Gaur[141], L. Gauthier[95], P. Gauzzi[132a,132b], I.L. Gavrilenko[96], C. Gay[168], G. Gaycken[21], E.N. Gazis[10], P. Ge[33d], Z. Gecse[168],

C.N.P. Gee[131], D.A.A. Geerts[107], Ch. Geich-Gimbel[21], M.P. Geisler[58a], C. Gemme[50a], M.H. Genest[55], S. Gentile[132a,132b], M. George[54], S. George[77], D. Gerbaudo[163], A. Gershon[153], H. Ghazlane[135b], B. Giacobbe[20a], S. Giagu[132a,132b], V. Giangiobbe[12], P. Giannetti[124a,124b], B. Gibbard[25], S.M. Gibson[77], M. Gilchriese[15], T.P.S. Gillam[28], D. Gillberg[30], G. Gilles[34], D.M. Gingrich[3,d], N. Giokaris[9], M.P. Giordani[164a,164c], F.M. Giorgi[20a], F.M. Giorgi[16], P.F. Giraud[136], P. Giromini[47], D. Giugni[91a], C. Giuliani[48], M. Giulini[58b], B.K. Gjelsten[119], S. Gkaitatzis[154], I. Gkialas[154], E.L. Gkougkousis[117], L.K. Gladilin[99], C. Glasman[82], J. Glatzer[30], P.C.F. Glaysher[46], A. Glazov[42], M. Goblirsch-Kolb[101], J.R. Goddard[76], J. Godlewski[39], S. Goldfarb[89], T. Golling[49], D. Golubkov[130], A. Gomes[126a,126b,126d], R. Gonçalo[126a], J. Goncalves Pinto Firmino Da Costa[136], L. Gonella[21], S. González de la Hoz[167], G. Gonzalez Parra[12], S. Gonzalez-Sevilla[49], L. Goossens[30], P.A. Gorbounov[97], H.A. Gordon[25], I. Gorelov[105], B. Gorini[30], E. Gorini[73a,73b], A. Gorišek[75], E. Gornicki[39], A.T. Goshaw[45], C. Gössling[43], M.I. Gostkin[65], D. Goujdami[135c], A.G. Goussiou[138], N. Govender[145b], E. Gozani[152], H.M.X. Grabas[137], L. Graber[54], I. Grabowska-Bold[38a], P. Grafström[20a,20b], K-J. Grahn[42], J. Gramling[49], E. Gramstad[119], S. Grancagnolo[16], V. Grassi[148], V. Gratchev[123], H.M. Gray[30], E. Graziani[134a], Z.D. Greenwood[79,n], K. Gregersen[78], I.M. Gregor[42], P. Grenier[143], J. Griffiths[8], A.A. Grillo[137], K. Grimm[72], S. Grinstein[12,o], Ph. Gris[34], J.-F. Grivaz[117], J.P. Grohs[44], A. Grohsjean[42], E. Gross[172], J. Grosse-Knetter[54], G.C. Grossi[79], Z.J. Grout[149], L. Guan[33b], J. Guenther[128], F. Guescini[49], D. Guest[176], O. Gueta[153], E. Guido[50a,50b], T. Guillemin[117], S. Guindon[2], U. Gul[53], C. Gumpert[44], J. Guo[33e], S. Gupta[120], G. Gustavino[132a,132b], P. Gutierrez[113], N.G. Gutierrez Ortiz[53], C. Gutschow[44], C. Guyot[136], C. Gwenlan[120], C.B. Gwilliam[74], A. Haas[110], C. Haber[15], H.K. Hadavand[8], N. Haddad[135e], P. Haefner[21], S. Hageböck[21], Z. Hajduk[39], H. Hakobyan[177], M. Haleem[42], J. Haley[114], D. Hall[120], G. Halladjian[90], G.D. Hallewell[85], K. Hamacher[175], P. Hamal[115], K. Hamano[169], M. Hamer[54], A. Hamilton[145a], G.N. Hamity[145c], P.G. Hamnett[42], L. Han[33b], K. Hanagaki[118], K. Hanawa[155], M. Hance[15], P. Hanke[58a], R. Hanna[136], J.B. Hansen[36], J.D. Hansen[36], M.C. Hansen[21], P.H. Hansen[36], K. Hara[160], A.S. Hard[173], T. Harenberg[175], F. Hariri[117], S. Harkusha[92], R.D. Harrington[46], P.F. Harrison[170], F. Hartjes[107], M. Hasegawa[67], S. Hasegawa[103], Y. Hasegawa[140], A. Hasib[113], S. Hassani[136], S. Haug[17], R. Hauser[90], L. Hauswald[44], M. Havranek[127], C.M. Hawkes[18], R.J. Hawkings[30], A.D. Hawkins[81], T. Hayashi[160], D. Hayden[90], C.P. Hays[120], J.M. Hays[76], H.S. Hayward[74], S.J. Haywood[131], S.J. Head[18], T. Heck[83], V. Hedberg[81], L. Heelan[8], S. Heim[122], T. Heim[175], B. Heinemann[15], L. Heinrich[110], J. Hejbal[127], L. Helary[22], S. Hellman[146a,146b], D. Hellmich[21], C. Helsens[30], J. Henderson[120], R.C.W. Henderson[72], Y. Heng[173], C. Hengler[42], A. Henrichs[176], A.M. Henriques Correia[30], S. Henrot-Versille[117], G.H. Herbert[16], Y. Hernández Jiménez[167], R. Herrberg-Schubert[16], G. Herten[48], R. Hertenberger[100], L. Hervas[30], G.G. Hesketh[78], N.P. Hessey[107], J.W. Hetherly[40], R. Hickling[76], E. Higón-Rodriguez[167], E. Hill[169], J.C. Hill[28], K.H. Hiller[42], S.J. Hillier[18], I. Hinchliffe[15], E. Hines[122], R.R. Hinman[15], M. Hirose[157], D. Hirschbuehl[175], J. Hobbs[148], N. Hod[107], M.C. Hodgkinson[139], P. Hodgson[139], A. Hoecker[30], M.R. Hoeferkamp[105], F. Hoenig[100], M. Hohlfeld[83], D. Hohn[21], T.R. Holmes[15], M. Homann[43], T.M. Hong[125], L. Hooft van Huysduynen[110], W.H. Hopkins[116], Y. Horii[103], A.J. Horton[142], J-Y. Hostachy[55], S. Hou[151], A. Hoummada[135a], J. Howard[120], J. Howarth[42], M. Hrabovsky[115], I. Hristova[16], J. Hrivnac[117], T. Hryn'ova[5], A. Hrynevich[93], C. Hsu[145c], P.J. Hsu[151,p], S.-C. Hsu[138], D. Hu[35], Q. Hu[33b], X. Hu[89], Y. Huang[42], Z. Hubacek[30], F. Hubaut[85], F. Huegging[21], T.B. Huffman[120], E.W. Hughes[35], G. Hughes[72], M. Huhtinen[30], T.A. Hülsing[83], N. Huseynov[65,b], J. Huston[90], J. Huth[57], G. Iacobucci[49], G. Iakovidis[25], I. Ibragimov[141], L. Iconomidou-Fayard[117], E. Ideal[176], Z. Idrissi[135e], P. Iengo[30], O. Igonkina[107], T. Iizawa[171], Y. Ikegami[66], M. Ikeno[66], Y. Ilchenko[31,q], D. Iliadis[154], N. Ilic[143], Y. Inamaru[67], T. Ince[101], P. Ioannou[9], M. Iodice[134a], K. Iordanidou[35], V. Ippolito[57], A. Irles Quiles[167], C. Isaksson[166], M. Ishino[68], M. Ishitsuka[157], R. Ishmukhametov[111], C. Issever[120], S. Istin[19a], J.M. Iturbe Ponce[84], R. Iuppa[133a,133b], J. Ivarsson[81], W. Iwanski[39], H. Iwasaki[66], J.M. Izen[41], V. Izzo[104a], S. Jabbar[3], B. Jackson[122], M. Jackson[74], P. Jackson[1], M.R. Jaekel[30], V. Jain[2], K. Jakobs[48],

S. Jakobsen[30], T. Jakoubek[127], J. Jakubek[128], D.O. Jamin[151], D.K. Jana[79], E. Jansen[78], R. Jansky[62], J. Janssen[21], M. Janus[170], G. Jarlskog[81], N. Javadov[65,b], T. Javůrek[48], L. Jeanty[15], J. Jejelava[51a,r], G.-Y. Jeng[150], D. Jennens[88], P. Jenni[48,s], J. Jentzsch[43], C. Jeske[170], S. Jézéquel[5], H. Ji[173], J. Jia[148], Y. Jiang[33b], S. Jiggins[78], J. Jimenez Pena[167], S. Jin[33a], A. Jinaru[26a], O. Jinnouchi[157], M.D. Joergensen[36], P. Johansson[139], K.A. Johns[7], K. Jon-And[146a,146b], G. Jones[170], R.W.L. Jones[72], T.J. Jones[74], J. Jongmanns[58a], P.M. Jorge[126a,126b], K.D. Joshi[84], J. Jovicevic[159a], X. Ju[173], C.A. Jung[43], P. Jussel[62], A. Juste Rozas[12,o], M. Kaci[167], A. Kaczmarska[39], M. Kado[117], H. Kagan[111], M. Kagan[143], S.J. Kahn[85], E. Kajomovitz[45], C.W. Kalderon[120], S. Kama[40], A. Kamenshchikov[130], N. Kanaya[155], M. Kaneda[30], S. Kaneti[28], V.A. Kantserov[98], J. Kanzaki[66], B. Kaplan[110], A. Kapliy[31], D. Kar[53], K. Karakostas[10], A. Karamaoun[3], N. Karastathis[10,107], M.J. Kareem[54], M. Karnevskiy[83], S.N. Karpov[65], Z.M. Karpova[65], K. Karthik[110], V. Kartvelishvili[72], A.N. Karyukhin[130], L. Kashif[173], R.D. Kass[111], A. Kastanas[14], Y. Kataoka[155], A. Katre[49], J. Katzy[42], K. Kawagoe[70], T. Kawamoto[155], G. Kawamura[54], S. Kazama[155], V.F. Kazanin[109,c], M.Y. Kazarinov[65], R. Keeler[169], R. Kehoe[40], J.S. Keller[42], J.J. Kempster[77], H. Keoshkerian[84], O. Kepka[127], B.P. Kerševan[75], S. Kersten[175], R.A. Keyes[87], F. Khalil-zada[11], H. Khandanyan[146a,146b], A. Khanov[114], A.G. Kharlamov[109,c], T.J. Khoo[28], V. Khovanskiy[97], E. Khramov[65], J. Khubua[51b,t], H.Y. Kim[8], H. Kim[146a,146b], S.H. Kim[160], Y.K. Kim[31], N. Kimura[154], O.M. Kind[16], B.T. King[74], M. King[167], S.B. King[168], J. Kirk[131], A.E. Kiryunin[101], T. Kishimoto[67], D. Kisielewska[38a], F. Kiss[48], K. Kiuchi[160], O. Kivernyk[136], E. Kladiva[144b], M.H. Klein[35], M. Klein[74], U. Klein[74], K. Kleinknecht[83], P. Klimek[146a,146b], A. Klimentov[25], R. Klingenberg[43], J.A. Klinger[139], T. Klioutchnikova[30], E.-E. Kluge[58a], P. Kluit[107], S. Kluth[101], E. Kneringer[62], E.B.F.G. Knoops[85], A. Knue[53], A. Kobayashi[155], D. Kobayashi[157], T. Kobayashi[155], M. Kobel[44], M. Kocian[143], P. Kodys[129], T. Koffas[29], E. Koffeman[107], L.A. Kogan[120], S. Kohlmann[175], Z. Kohout[128], T. Kohriki[66], T. Koi[143], H. Kolanoski[16], I. Koletsou[5], A.A. Komar[96,*], Y. Komori[155], T. Kondo[66], N. Kondrashova[42], K. Köneke[48], A.C. König[106], S. König[83], T. Kono[66,u], R. Konoplich[110,v], N. Konstantinidis[78], R. Kopeliansky[152], S. Koperny[38a], L. Köpke[83], A.K. Kopp[48], K. Korcyl[39], K. Kordas[154], A. Korn[78], A.A. Korol[109,c], I. Korolkov[12], E.V. Korolkova[139], O. Kortner[101], S. Kortner[101], T. Kosek[129], V.V. Kostyukhin[21], V.M. Kotov[65], A. Kotwal[45], A. Kourkoumeli-Charalampidi[154], C. Kourkoumelis[9], V. Kouskoura[25], A. Koutsman[159a], R. Kowalewski[169], T.Z. Kowalski[38a], W. Kozanecki[136], A.S. Kozhin[130], V.A. Kramarenko[99], G. Kramberger[75], D. Krasnopevtsev[98], M.W. Krasny[80], A. Krasznahorkay[30], J.K. Kraus[21], A. Kravchenko[25], S. Kreiss[110], M. Kretz[58c], J. Kretzschmar[74], K. Kreutzfeldt[52], P. Krieger[158], K. Krizka[31], K. Kroeninger[43], H. Kroha[101], J. Kroll[122], J. Kroseberg[21], J. Krstic[13], U. Kruchonak[65], H. Krüger[21], N. Krumnack[64], Z.V. Krumshteyn[65], A. Kruse[173], M.C. Kruse[45], M. Kruskal[22], T. Kubota[88], H. Kucuk[78], S. Kuday[4b], S. Kuehn[48], A. Kugel[58c], F. Kuger[174], A. Kuhl[137], T. Kuhl[42], V. Kukhtin[65], Y. Kulchitsky[92], S. Kuleshov[32b], M. Kuna[132a,132b], T. Kunigo[68], A. Kupco[127], H. Kurashige[67], Y.A. Kurochkin[92], R. Kurumida[67], V. Kus[127], E.S. Kuwertz[169], M. Kuze[157], J. Kvita[115], T. Kwan[169], D. Kyriazopoulos[139], A. La Rosa[49], J.L. La Rosa Navarro[24d], L. La Rotonda[37a,37b], C. Lacasta[167], F. Lacava[132a,132b], J. Lacey[29], H. Lacker[16], D. Lacour[80], V.R. Lacuesta[167], E. Ladygin[65], R. Lafaye[5], B. Laforge[80], T. Lagouri[176], S. Lai[48], L. Lambourne[78], S. Lammers[61], C.L. Lampen[7], W. Lampl[7], E. Lançon[136], U. Landgraf[48], M.P.J. Landon[76], V.S. Lang[58a], J.C. Lange[12], A.J. Lankford[163], F. Lanni[25], K. Lantzsch[30], S. Laplace[80], C. Lapoire[30], J.F. Laporte[136], T. Lari[91a], F. Lasagni Manghi[20a,20b], M. Lassnig[30], P. Laurelli[47], W. Lavrijsen[15], A.T. Law[137], P. Laycock[74], T. Lazovich[57], O. Le Dortz[80], E. Le Guirriec[85], E. Le Menedeu[12], M. LeBlanc[169], T. LeCompte[6], F. Ledroit-Guillon[55], C.A. Lee[145b], S.C. Lee[151], L. Lee[1], G. Lefebvre[80], M. Lefebvre[169], F. Legger[100], C. Leggett[15], A. Lehan[74], G. Lehmann Miotto[30], X. Lei[7], W.A. Leight[29], A. Leisos[154,w], A.G. Leister[176], M.A.L. Leite[24d], R. Leitner[129], D. Lellouch[172], B. Lemmer[54], K.J.C. Leney[78], T. Lenz[21], B. Lenzi[30], R. Leone[7], S. Leone[124a,124b], C. Leonidopoulos[46], S. Leontsinis[10], C. Leroy[95], C.G. Lester[28], M. Levchenko[123], J. Levêque[5], D. Levin[89], L.J. Levinson[172],

M. Levy[18], A. Lewis[120], A.M. Leyko[21], M. Leyton[41], B. Li[33b,x], H. Li[148], H.L. Li[31], L. Li[45], L. Li[33e], S. Li[45], Y. Li[33c,y], Z. Liang[137], H. Liao[34], B. Liberti[133a], A. Liblong[158], P. Lichard[30], K. Lie[165], J. Liebal[21], W. Liebig[14], C. Limbach[21], A. Limosani[150], S.C. Lin[151,z], T.H. Lin[83], F. Linde[107], B.E. Lindquist[148], J.T. Linnemann[90], E. Lipeles[122], A. Lipniacka[14], M. Lisovyi[58b], T.M. Liss[165], D. Lissauer[25], A. Lister[168], A.M. Litke[137], B. Liu[151,aa], D. Liu[151], H. Liu[89], J. Liu[85], J.B. Liu[33b], K. Liu[85], L. Liu[165], M. Liu[45], M. Liu[33b], Y. Liu[33b], M. Livan[121a,121b], A. Lleres[55], J. Llorente Merino[82], S.L. Lloyd[76], F. Lo Sterzo[151], E. Lobodzinska[42], P. Loch[7], W.S. Lockman[137], F.K. Loebinger[84], A.E. Loevschall-Jensen[36], A. Loginov[176], T. Lohse[16], K. Lohwasser[42], M. Lokajicek[127], B.A. Long[22], J.D. Long[89], R.E. Long[72], K.A. Looper[111], L. Lopes[126a], D. Lopez Mateos[57], B. Lopez Paredes[139], I. Lopez Paz[12], J. Lorenz[100], N. Lorenzo Martinez[61], M. Losada[162], P. Loscutoff[15], P.J. Lösel[100], X. Lou[33a], A. Lounis[117], J. Love[6], P.A. Love[72], N. Lu[89], H.J. Lubatti[138], C. Luci[132a,132b], A. Lucotte[55], F. Luehring[61], W. Lukas[62], L. Luminari[132a], O. Lundberg[146a,146b], B. Lund-Jensen[147], D. Lynn[25], R. Lysak[127], E. Lytken[81], H. Ma[25], L.L. Ma[33d], G. Maccarrone[47], A. Macchiolo[101], C.M. Macdonald[139], J. Machado Miguens[122,126b], D. Macina[30], D. Madaffari[85], R. Madar[34], H.J. Maddocks[72], W.F. Mader[44], A. Madsen[166], S. Maeland[14], T. Maeno[25], A. Maevskiy[99], E. Magradze[54], K. Mahboubi[48], J. Mahlstedt[107], C. Maiani[136], C. Maidantchik[24a], A.A. Maier[101], T. Maier[100], A. Maio[126a,126b,126d], S. Majewski[116], Y. Makida[66], N. Makovec[117], B. Malaescu[80], Pa. Malecki[39], V.P. Maleev[123], F. Malek[55], U. Mallik[63], D. Malon[6], C. Malone[143], S. Maltezos[10], V.M. Malyshev[109], S. Malyukov[30], J. Mamuzic[42], G. Mancini[47], B. Mandelli[30], L. Mandelli[91a], I. Mandić[75], R. Mandrysch[63], J. Maneira[126a,126b], A. Manfredini[101], L. Manhaes de Andrade Filho[24b], J. Manjarres Ramos[159b], A. Mann[100], P.M. Manning[137], A. Manousakis-Katsikakis[9], B. Mansoulie[136], R. Mantifel[87], M. Mantoani[54], L. Mapelli[30], L. March[145c], G. Marchiori[80], M. Marcisovsky[127], C.P. Marino[169], M. Marjanovic[13], D.E. Marley[89], F. Marroquim[24a], S.P. Marsden[84], Z. Marshall[15], L.F. Marti[17], S. Marti-Garcia[167], B. Martin[90], T.A. Martin[170], V.J. Martin[46], B. Martin dit Latour[14], M. Martinez[12,o], S. Martin-Haugh[131], V.S. Martoiu[26a], A.C. Martyniuk[78], M. Marx[138], F. Marzano[132a], A. Marzin[30], L. Masetti[83], T. Mashimo[155], R. Mashinistov[96], J. Masik[84], A.L. Maslennikov[109,c], I. Massa[20a,20b], L. Massa[20a,20b], N. Massol[5], P. Mastrandrea[148], A. Mastroberardino[37a,37b], T. Masubuchi[155], P. Mättig[175], J. Mattmann[83], J. Maurer[26a], S.J. Maxfield[74], D.A. Maximov[109,c], R. Mazini[151], S.M. Mazza[91a,91b], L. Mazzaferro[133a,133b], G. Mc Goldrick[158], S.P. Mc Kee[89], A. McCarn[89], R.L. McCarthy[148], T.G. McCarthy[29], N.A. McCubbin[131], K.W. McFarlane[56,*], J.A. Mcfayden[78], G. Mchedlidze[54], S.J. McMahon[131], R.A. McPherson[169,k], M. Medinnis[42], S. Meehan[145a], S. Mehlhase[100], A. Mehta[74], K. Meier[58a], C. Meineck[100], B. Meirose[41], B.R. Mellado Garcia[145c], F. Meloni[17], A. Mengarelli[20a,20b], S. Menke[101], E. Meoni[161], K.M. Mercurio[57], S. Mergelmeyer[21], P. Mermod[49], L. Merola[104a,104b], C. Meroni[91a], F.S. Merritt[31], A. Messina[132a,132b], J. Metcalfe[25], A.S. Mete[163], C. Meyer[83], C. Meyer[122], J-P. Meyer[136], J. Meyer[107], R.P. Middleton[131], S. Miglioranzi[164a,164c], L. Mijović[21], G. Mikenberg[172], M. Mikestikova[127], M. Mikuž[75], M. Milesi[88], A. Milic[30], D.W. Miller[31], C. Mills[46], A. Milov[172], D.A. Milstead[146a,146b], A.A. Minaenko[130], Y. Minami[155], I.A. Minashvili[65], A.I. Mincer[110], B. Mindur[38a], M. Mineev[65], Y. Ming[173], L.M. Mir[12], T. Mitani[171], J. Mitrevski[100], V.A. Mitsou[167], A. Miucci[49], P.S. Miyagawa[139], J.U. Mjörnmark[81], T. Moa[146a,146b], K. Mochizuki[85], S. Mohapatra[35], W. Mohr[48], S. Molander[146a,146b], R. Moles-Valls[167], K. Mönig[42], C. Monini[55], J. Monk[36], E. Monnier[85], J. Montejo Berlingen[12], F. Monticelli[71], S. Monzani[132a,132b], R.W. Moore[3], N. Morange[117], D. Moreno[162], M. Moreno Llácer[54], P. Morettini[50a], M. Morgenstern[44], M. Morii[57], M. Morinaga[155], V. Morisbak[119], S. Moritz[83], A.K. Morley[147], G. Mornacchi[30], J.D. Morris[76], S.S. Mortensen[36], A. Morton[53], L. Morvaj[103], M. Mosidze[51b], J. Moss[111], K. Motohashi[157], R. Mount[143], E. Mountricha[25], S.V. Mouraviev[96,*], E.J.W. Moyse[86], S. Muanza[85], R.D. Mudd[18], F. Mueller[101], J. Mueller[125], K. Mueller[21], R.S.P. Mueller[100], T. Mueller[28], D. Muenstermann[49], P. Mullen[53], G.A. Mullier[17], Y. Munwes[153], J.A. Murillo Quijada[18], W.J. Murray[170,131], H. Musheghyan[54], E. Musto[152],

A.G. Myagkov[130,ab], M. Myska[128], O. Nackenhorst[54], J. Nadal[54], K. Nagai[120], R. Nagai[157], Y. Nagai[85], K. Nagano[66], A. Nagarkar[111], Y. Nagasaka[59], K. Nagata[160], M. Nagel[101], E. Nagy[85], A.M. Nairz[30], Y. Nakahama[30], K. Nakamura[66], T. Nakamura[155], I. Nakano[112], H. Namasivayam[41], R.F. Naranjo Garcia[42], R. Narayan[31], T. Naumann[42], G. Navarro[162], R. Nayyar[7], H.A. Neal[89], P.Yu. Nechaeva[96], T.J. Neep[84], P.D. Nef[143], A. Negri[121a,121b], M. Negrini[20a], S. Nektarijevic[106], C. Nellist[117], A. Nelson[163], S. Nemecek[127], P. Nemethy[110], A.A. Nepomuceno[24a], M. Nessi[30,ac], M.S. Neubauer[165], M. Neumann[175], R.M. Neves[110], P. Nevski[25], P.R. Newman[18], D.H. Nguyen[6], R.B. Nickerson[120], R. Nicolaidou[136], B. Nicquevert[30], J. Nielsen[137], N. Nikiforou[35], A. Nikiforov[16], V. Nikolaenko[130,ab], I. Nikolic-Audit[80], K. Nikolopoulos[18], J.K. Nilsen[119], P. Nilsson[25], Y. Ninomiya[155], A. Nisati[132a], R. Nisius[101], T. Nobe[157], L. Nodulman[6], M. Nomachi[118], I. Nomidis[29], T. Nooney[76], S. Norberg[113], M. Nordberg[30], O. Novgorodova[44], S. Nowak[101], M. Nozaki[66], L. Nozka[115], K. Ntekas[10], G. Nunes Hanninger[88], T. Nunnemann[100], E. Nurse[78], F. Nuti[88], B.J. O'Brien[46], F. O'grady[7], D.C. O'Neil[142], V. O'Shea[53], F.G. Oakham[29,d], H. Oberlack[101], T. Obermann[21], J. Ocariz[80], A. Ochi[67], I. Ochoa[78], J.P. Ochoa-Ricoux[32a], S. Oda[70], S. Odaka[66], H. Ogren[61], A. Oh[84], S.H. Oh[45], C.C. Ohm[15], H. Ohman[166], H. Oide[30], W. Okamura[118], H. Okawa[160], Y. Okumura[31], T. Okuyama[155], A. Olariu[26a], S.A. Olivares Pino[46], D. Oliveira Damazio[25], E. Oliver Garcia[167], A. Olszewski[39], J. Olszowska[39], A. Onofre[126a,126e], P.U.E. Onyisi[31,q], C.J. Oram[159a], M.J. Oreglia[31], Y. Oren[153], D. Orestano[134a,134b], N. Orlando[154], C. Oropeza Barrera[53], R.S. Orr[158], B. Osculati[50a,50b], R. Ospanov[84], G. Otero y Garzon[27], H. Otono[70], M. Ouchrif[135d], E.A. Ouellette[169], F. Ould-Saada[119], A. Ouraou[136], K.P. Oussoren[107], Q. Ouyang[33a], A. Ovcharova[15], M. Owen[53], R.E. Owen[18], V.E. Ozcan[19a], N. Ozturk[8], K. Pachal[142], A. Pacheco Pages[12], C. Padilla Aranda[12], M. Pagáčová[48], S. Pagan Griso[15], E. Paganis[139], C. Pahl[101], F. Paige[25], P. Pais[86], K. Pajchel[119], G. Palacino[159b], S. Palestini[30], M. Palka[38b], D. Pallin[34], A. Palma[126a,126b], Y.B. Pan[173], E.St. Panagiotopoulou[10], C.E. Pandini[80], J.G. Panduro Vazquez[77], P. Pani[146a,146b], S. Panitkin[25], D. Pantea[26a], L. Paolozzi[49], Th.D. Papadopoulou[10], K. Papageorgiou[154], A. Paramonov[6], D. Paredes Hernandez[154], M.A. Parker[28], K.A. Parker[139], F. Parodi[50a,50b], J.A. Parsons[35], U. Parzefall[48], E. Pasqualucci[132a], S. Passaggio[50a], F. Pastore[134a,134b,*], Fr. Pastore[77], G. Pásztor[29], S. Pataraia[175], N.D. Patel[150], J.R. Pater[84], T. Pauly[30], J. Pearce[169], B. Pearson[113], L.E. Pedersen[36], M. Pedersen[119], S. Pedraza Lopez[167], R. Pedro[126a,126b], S.V. Peleganchuk[109,c], D. Pelikan[166], H. Peng[33b], B. Penning[31], J. Penwell[61], D.V. Perepelitsa[25], E. Perez Codina[159a], M.T. Pérez García-Estañ[167], L. Perini[91a,91b], H. Pernegger[30], S. Perrella[104a,104b], R. Peschke[42], V.D. Peshekhonov[65], K. Peters[30], R.F.Y. Peters[84], B.A. Petersen[30], T.C. Petersen[36], E. Petit[42], A. Petridis[146a,146b], C. Petridou[154], E. Petrolo[132a], F. Petrucci[134a,134b], N.E. Pettersson[157], R. Pezoa[32b], P.W. Phillips[131], G. Piacquadio[143], E. Pianori[170], A. Picazio[49], E. Piccaro[76], M. Piccinini[20a,20b], M.A. Pickering[120], R. Piegaia[27], D.T. Pignotti[111], J.E. Pilcher[31], A.D. Pilkington[84], J. Pina[126a,126b,126d], M. Pinamonti[164a,164c,ad], J.L. Pinfold[3], A. Pingel[36], B. Pinto[126a], S. Pires[80], H. Pirumov[42], M. Pitt[172], C. Pizio[91a,91b], L. Plazak[144a], M.-A. Pleier[25], V. Pleskot[129], E. Plotnikova[65], P. Plucinski[146a,146b], D. Pluth[64], R. Poettgen[146a,146b], L. Poggioli[117], D. Pohl[21], G. Polesello[121a], A. Poley[42], A. Policicchio[37a,37b], R. Polifka[158], A. Polini[20a], C.S. Pollard[53], V. Polychronakos[25], K. Pommès[30], L. Pontecorvo[132a], B.G. Pope[90], G.A. Popeneciu[26b], D.S. Popovic[13], A. Poppleton[30], S. Pospisil[128], K. Potamianos[15], I.N. Potrap[65], C.J. Potter[149], C.T. Potter[116], G. Poulard[30], J. Poveda[30], V. Pozdnyakov[65], P. Pralavorio[85], A. Pranko[15], S. Prasad[30], S. Prell[64], D. Price[84], L.E. Price[6], M. Primavera[73a], S. Prince[87], M. Proissl[46], K. Prokofiev[60c], F. Prokoshin[32b], E. Protopapadaki[136], S. Protopopescu[25], J. Proudfoot[6], M. Przybycien[38a], E. Ptacek[116], D. Puddu[134a,134b], E. Pueschel[86], D. Puldon[148], M. Purohit[25,ae], P. Puzo[117], J. Qian[89], G. Qin[53], Y. Qin[84], A. Quadt[54], D.R. Quarrie[15], W.B. Quayle[164a,164b], M. Queitsch-Maitland[84], D. Quilty[53], S. Raddum[119], V. Radeka[25], V. Radescu[42], S.K. Radhakrishnan[148], P. Radloff[116], P. Rados[88], F. Ragusa[91a,91b], G. Rahal[178], S. Rajagopalan[25], M. Rammensee[30], C. Rangel-Smith[166], F. Rauscher[100], S. Rave[83], T. Ravenscroft[53], M. Raymond[30],

A.L. Read[119], N.P. Readioff[74], D.M. Rebuzzi[121a,121b], A. Redelbach[174], G. Redlinger[25], R. Reece[137], K. Reeves[41], L. Rehnisch[16], H. Reisin[27], M. Relich[163], C. Rembser[30], H. Ren[33a], A. Renaud[117], M. Rescigno[132a], S. Resconi[91a], O.L. Rezanova[109,c], P. Reznicek[129], R. Rezvani[95], R. Richter[101], S. Richter[78], E. Richter-Was[38b], O. Ricken[21], M. Ridel[80], P. Rieck[16], C.J. Riegel[175], J. Rieger[54], M. Rijssenbeek[148], A. Rimoldi[121a,121b], L. Rinaldi[20a], B. Ristić[49], E. Ritsch[30], I. Riu[12], F. Rizatdinova[114], E. Rizvi[76], S.H. Robertson[87,k], A. Robichaud-Veronneau[87], D. Robinson[28], J.E.M. Robinson[84], A. Robson[53], C. Roda[124a,124b], S. Roe[30], O. Røhne[119], S. Rolli[161], A. Romaniouk[98], M. Romano[20a,20b], S.M. Romano Saez[34], E. Romero Adam[167], N. Rompotis[138], M. Ronzani[48], L. Roos[80], E. Ros[167], S. Rosati[132a], K. Rosbach[48], P. Rose[137], P.L. Rosendahl[14], O. Rosenthal[141], V. Rossetti[146a,146b], E. Rossi[104a,104b], L.P. Rossi[50a], R. Rosten[138], M. Rotaru[26a], I. Roth[172], J. Rothberg[138], D. Rousseau[117], C.R. Royon[136], A. Rozanov[85], Y. Rozen[152], X. Ruan[145c], F. Rubbo[143], I. Rubinskiy[42], V.I. Rud[99], C. Rudolph[44], M.S. Rudolph[158], F. Rühr[48], A. Ruiz-Martinez[30], Z. Rurikova[48], N.A. Rusakovich[65], A. Ruschke[100], H.L. Russell[138], J.P. Rutherfoord[7], N. Ruthmann[48], Y.F. Ryabov[123], M. Rybar[165], G. Rybkin[117], N.C. Ryder[120], A.F. Saavedra[150], G. Sabato[107], S. Sacerdoti[27], A. Saddique[3], H.F-W. Sadrozinski[137], R. Sadykov[65], F. Safai Tehrani[132a], M. Saimpert[136], H. Sakamoto[155], Y. Sakurai[171], G. Salamanna[134a,134b], A. Salamon[133a], M. Saleem[113], D. Salek[107], P.H. Sales De Bruin[138], D. Salihagic[101], A. Salnikov[143], J. Salt[167], D. Salvatore[37a,37b], F. Salvatore[149], A. Salvucci[106], A. Salzburger[30], D. Sampsonidis[154], A. Sanchez[104a,104b], J. Sánchez[167], V. Sanchez Martinez[167], H. Sandaker[119], R.L. Sandbach[76], H.G. Sander[83], M.P. Sanders[100], M. Sandhoff[175], C. Sandoval[162], R. Sandstroem[101], D.P.C. Sankey[131], M. Sannino[50a,50b], A. Sansoni[47], C. Santoni[34], R. Santonico[133a,133b], H. Santos[126a], I. Santoyo Castillo[149], K. Sapp[125], A. Sapronov[65], J.G. Saraiva[126a,126d], B. Sarrazin[21], O. Sasaki[66], Y. Sasaki[155], K. Sato[160], G. Sauvage[5,*], E. Sauvan[5], G. Savage[77], P. Savard[158,d], C. Sawyer[131], L. Sawyer[79,n], J. Saxon[31], C. Sbarra[20a], A. Sbrizzi[20a,20b], T. Scanlon[78], D.A. Scannicchio[163], M. Scarcella[150], V. Scarfone[37a,37b], J. Schaarschmidt[172], P. Schacht[101], D. Schaefer[30], R. Schaefer[42], J. Schaeffer[83], S. Schaepe[21], S. Schaetzel[58b], U. Schäfer[83], A.C. Schaffer[117], D. Schaile[100], R.D. Schamberger[148], V. Scharf[58a], V.A. Schegelsky[123], D. Scheirich[129], M. Schernau[163], C. Schiavi[50a,50b], C. Schillo[48], M. Schioppa[37a,37b], S. Schlenker[30], E. Schmidt[48], K. Schmieden[30], C. Schmitt[83], S. Schmitt[58b], S. Schmitt[42], B. Schneider[159a], Y.J. Schnellbach[74], U. Schnoor[44], L. Schoeffel[136], A. Schoening[58b], B.D. Schoenrock[90], E. Schopf[21], A.L.S. Schorlemmer[54], M. Schott[83], D. Schouten[159a], J. Schovancova[8], S. Schramm[49], M. Schreyer[174], C. Schroeder[83], N. Schuh[83], M.J. Schultens[21], H.-C. Schultz-Coulon[58a], H. Schulz[16], M. Schumacher[48], B.A. Schumm[137], Ph. Schune[136], C. Schwanenberger[84], A. Schwartzman[143], T.A. Schwarz[89], Ph. Schwegler[101], H. Schweiger[84], Ph. Schwemling[136], R. Schwienhorst[90], J. Schwindling[136], T. Schwindt[21], F.G. Sciacca[17], E. Scifo[117], G. Sciolla[23], F. Scuri[124a,124b], F. Scutti[21], J. Searcy[89], G. Sedov[42], E. Sedykh[123], P. Seema[21], S.C. Seidel[105], A. Seiden[137], F. Seifert[128], J.M. Seixas[24a], G. Sekhniaidze[104a], K. Sekhon[89], S.J. Sekula[40], D.M. Seliverstov[123,*], N. Semprini-Cesari[20a,20b], C. Serfon[30], L. Serin[117], L. Serkin[164a,164b], T. Serre[85], M. Sessa[134a,134b], R. Seuster[159a], H. Severini[113], T. Sfiligoj[75], F. Sforza[30], A. Sfyrla[30], E. Shabalina[54], M. Shamim[116], L.Y. Shan[33a], R. Shang[165], J.T. Shank[22], M. Shapiro[15], P.B. Shatalov[97], K. Shaw[164a,164b], S.M. Shaw[84], A. Shcherbakova[146a,146b], C.Y. Shehu[149], P. Sherwood[78], L. Shi[151,af], S. Shimizu[67], C.O. Shimmin[163], M. Shimojima[102], M. Shiyakova[65], A. Shmeleva[96], D. Shoaleh Saadi[95], M.J. Shochet[31], S. Shojaii[91a,91b], S. Shrestha[111], E. Shulga[98], M.A. Shupe[7], S. Shushkevich[42], P. Sicho[127], O. Sidiropoulou[174], D. Sidorov[114], A. Sidoti[20a,20b], F. Siegert[44], Dj. Sijacki[13], J. Silva[126a,126d], Y. Silver[153], S.B. Silverstein[146a], V. Simak[128], O. Simard[5], Lj. Simic[13], S. Simion[117], E. Simioni[83], B. Simmons[78], D. Simon[34], R. Simoniello[91a,91b], P. Sinervo[158], N.B. Sinev[116], G. Siragusa[174], A.N. Sisakyan[65,*], S.Yu. Sivoklokov[99], J. Sjölin[146a,146b], T.B. Sjursen[14], M.B. Skinner[72], H.P. Skottowe[57], P. Skubic[113], M. Slater[18], T. Slavicek[128], M. Slawinska[107], K. Sliwa[161], V. Smakhtin[172], B.H. Smart[46], L. Smestad[14],

S.Yu. Smirnov[98], Y. Smirnov[98], L.N. Smirnova[99,ag], O. Smirnova[81], M.N.K. Smith[35], R.W. Smith[35], M. Smizanska[72], K. Smolek[128], A.A. Snesarev[96], G. Snidero[76], S. Snyder[25], R. Sobie[169,k], F. Socher[44], A. Soffer[153], D.A. Soh[151,af], C.A. Solans[30], M. Solar[128], J. Solc[128], E.Yu. Soldatov[98], U. Soldevila[167], A.A. Solodkov[130], A. Soloshenko[65], O.V. Solovyanov[130], V. Solovyev[123], P. Sommer[48], H.Y. Song[33b,x], N. Soni[1], A. Sood[15], A. Sopczak[128], B. Sopko[128], V. Sopko[128], V. Sorin[12], D. Sosa[58b], M. Sosebee[8], C.L. Sotiropoulou[124a,124b], R. Soualah[164a,164c], A.M. Soukharev[109,c], D. South[42], B.C. Sowden[77], S. Spagnolo[73a,73b], M. Spalla[124a,124b], F. Spanò[77], W.R. Spearman[57], F. Spettel[101], R. Spighi[20a], G. Spigo[30], L.A. Spiller[88], M. Spousta[129], T. Spreitzer[158], R.D. St. Denis[53,*], S. Staerz[44], J. Stahlman[122], R. Stamen[58a], S. Stamm[16], E. Stanecka[39], R.W. Stanek[6], C. Stanescu[134a], M. Stanescu-Bellu[42], M.M. Stanitzki[42], S. Stapnes[119], E.A. Starchenko[130], J. Stark[55], P. Staroba[127], P. Starovoitov[42], R. Staszewski[39], P. Stavina[144a,*], P. Steinberg[25], B. Stelzer[142], H.J. Stelzer[30], O. Stelzer-Chilton[159a], H. Stenzel[52], S. Stern[101], G.A. Stewart[53], J.A. Stillings[21], M.C. Stockton[87], M. Stoebe[87], G. Stoicea[26a], P. Stolte[54], S. Stonjek[101], A.R. Stradling[8], A. Straessner[44], M.E. Stramaglia[17], J. Strandberg[147], S. Strandberg[146a,146b], A. Strandlie[119], E. Strauss[143], M. Strauss[113], P. Strizenec[144b], R. Ströhmer[174], D.M. Strom[116], R. Stroynowski[40], A. Strubig[106], S.A. Stucci[17], B. Stugu[14], N.A. Styles[42], D. Su[143], J. Su[125], R. Subramaniam[79], A. Succurro[12], Y. Sugaya[118], C. Suhr[108], M. Suk[128], V.V. Sulin[96], S. Sultansoy[4c], T. Sumida[68], S. Sun[57], X. Sun[33a], J.E. Sundermann[48], K. Suruliz[149], G. Susinno[37a,37b], M.R. Sutton[149], S. Suzuki[66], Y. Suzuki[66], M. Svatos[127], S. Swedish[168], M. Swiatlowski[143], I. Sykora[144a], T. Sykora[129], D. Ta[90], C. Taccini[134a,134b], K. Tackmann[42], J. Taenzer[158], A. Taffard[163], R. Tafirout[159a], N. Taiblum[153], H. Takai[25], R. Takashima[69], H. Takeda[67], T. Takeshita[140], Y. Takubo[66], M. Talby[85], A.A. Talyshev[109,c], J.Y.C. Tam[174], K.G. Tan[88], J. Tanaka[155], R. Tanaka[117], S. Tanaka[66], B.B. Tannenwald[111], N. Tannoury[21], S. Tapprogge[83], S. Tarem[152], F. Tarrade[29], G.F. Tartarelli[91a], P. Tas[129], M. Tasevsky[127], T. Tashiro[68], E. Tassi[37a,37b], A. Tavares Delgado[126a,126b], Y. Tayalati[135d], F.E. Taylor[94], G.N. Taylor[88], W. Taylor[159b], F.A. Teischinger[30], P. Teixeira-Dias[77], K.K. Temming[48], H. Ten Kate[30], P.K. Teng[151], J.J. Teoh[118], F. Tepel[175], S. Terada[66], K. Terashi[155], J. Terron[82], S. Terzo[101], M. Testa[47], R.J. Teuscher[158,k], J. Therhaag[21], T. Theveneaux-Pelzer[34], J.P. Thomas[18], J. Thomas-Wilsker[77], E.N. Thompson[35], P.D. Thompson[18], R.J. Thompson[84], A.S. Thompson[53], L.A. Thomsen[176], E. Thomson[122], M. Thomson[28], R.P. Thun[89,*], M.J. Tibbetts[15], R.E. Ticse Torres[85], V.O. Tikhomirov[96,ah], Yu.A. Tikhonov[109,c], S. Timoshenko[98], E. Tiouchichine[85], P. Tipton[176], S. Tisserant[85], T. Todorov[5,*], S. Todorova-Nova[129], J. Tojo[70], S. Tokár[144a], K. Tokushuku[66], K. Tollefson[90], E. Tolley[57], L. Tomlinson[84], M. Tomoto[103], L. Tompkins[143,ai], K. Toms[105], E. Torrence[116], H. Torres[142], E. Torró Pastor[167], J. Toth[85,aj], F. Touchard[85], D.R. Tovey[139], T. Trefzger[174], L. Tremblet[30], A. Tricoli[30], I.M. Trigger[159a], S. Trincaz-Duvoid[80], M.F. Tripiana[12], W. Trischuk[158], B. Trocmé[55], C. Troncon[91a], M. Trottier-McDonald[15], M. Trovatelli[169], P. True[90], L. Truong[164a,164c], M. Trzebinski[39], A. Trzupek[39], C. Tsarouchas[30], J.C-L. Tseng[120], P.V. Tsiareshka[92], D. Tsionou[154], G. Tsipolitis[10], N. Tsirintanis[9], S. Tsiskaridze[12], V. Tsiskaridze[48], E.G. Tskhadadze[51a], I.I. Tsukerman[97], V. Tsulaia[15], S. Tsuno[66], D. Tsybychev[148], A. Tudorache[26a], V. Tudorache[26a], A.N. Tuna[122], S.A. Tupputi[20a,20b], S. Turchikhin[99,ag], D. Turecek[128], R. Turra[91a,91b], A.J. Turvey[40], P.M. Tuts[35], A. Tykhonov[49], M. Tylmad[146a,146b], M. Tyndel[131], I. Ueda[155], R. Ueno[29], M. Ughetto[146a,146b], M. Ugland[14], M. Uhlenbrock[21], F. Ukegawa[160], G. Unal[30], A. Undrus[25], G. Unel[163], F.C. Ungaro[48], Y. Unno[66], C. Unverdorben[100], J. Urban[144b], P. Urquijo[88], P. Urrejola[83], G. Usai[8], A. Usanova[62], L. Vacavant[85], V. Vacek[128], B. Vachon[87], C. Valderanis[83], N. Valencic[107], S. Valentinetti[20a,20b], A. Valero[167], L. Valery[12], S. Valkar[129], E. Valladolid Gallego[167], S. Vallecorsa[49], J.A. Valls Ferrer[167], W. Van Den Wollenberg[107], P.C. Van Der Deijl[107], R. van der Geer[107], H. van der Graaf[107], R. Van Der Leeuw[107], N. van Eldik[152], P. van Gemmeren[6], J. Van Nieuwkoop[142], I. van Vulpen[107], M.C. van Woerden[30], M. Vanadia[132a,132b], W. Vandelli[30], R. Vanguri[122], A. Vaniachine[6], F. Vannucci[80], G. Vardanyan[177], R. Vari[132a], E.W. Varnes[7], T. Varol[40], D. Varouchas[80],

A. Vartapetian[8], K.E. Varvell[150], V.I. Vassilakopoulos[56], F. Vazeille[34], T. Vazquez Schroeder[87], J. Veatch[7], L.M. Veloce[158], F. Veloso[126a,126c], T. Velz[21], S. Veneziano[132a], A. Ventura[73a,73b], D. Ventura[86], M. Venturi[169], N. Venturi[158], A. Venturini[23], V. Vercesi[121a], M. Verducci[132a,132b], W. Verkerke[107], J.C. Vermeulen[107], A. Vest[44,ak], M.C. Vetterli[142,d], O. Viazlo[81], I. Vichou[165], T. Vickey[139], O.E. Vickey Boeriu[139], G.H.A. Viehhauser[120], S. Viel[15], R. Vigne[62], M. Villa[20a,20b], M. Villaplana Perez[91a,91b], E. Vilucchi[47], M.G. Vincter[29], V.B. Vinogradov[65], I. Vivarelli[149], F. Vives Vaque[3], S. Vlachos[10], D. Vladoiu[100], M. Vlasak[128], M. Vogel[32a], P. Vokac[128], G. Volpi[124a,124b], M. Volpi[88], H. von der Schmitt[101], H. von Radziewski[48], E. von Toerne[21], V. Vorobel[129], K. Vorobev[98], M. Vos[167], R. Voss[30], J.H. Vossebeld[74], N. Vranjes[13], M. Vranjes Milosavljevic[13], V. Vrba[127], M. Vreeswijk[107], R. Vuillermet[30], I. Vukotic[31], Z. Vykydal[128], P. Wagner[21], W. Wagner[175], H. Wahlberg[71], S. Wahrmund[44], J. Wakabayashi[103], J. Walder[72], R. Walker[100], W. Walkowiak[141], C. Wang[151], F. Wang[173], H. Wang[15], H. Wang[40], J. Wang[42], J. Wang[33a], K. Wang[87], R. Wang[6], S.M. Wang[151], T. Wang[21], X. Wang[176], C. Wanotayaroj[116], A. Warburton[87], C.P. Ward[28], D.R. Wardrope[78], M. Warsinsky[48], A. Washbrook[46], C. Wasicki[42], P.M. Watkins[18], A.T. Watson[18], I.J. Watson[150], M.F. Watson[18], G. Watts[138], S. Watts[84], B.M. Waugh[78], S. Webb[84], M.S. Weber[17], S.W. Weber[174], J.S. Webster[31], A.R. Weidberg[120], B. Weinert[61], J. Weingarten[54], C. Weiser[48], H. Weits[107], P.S. Wells[30], T. Wenaus[25], T. Wengler[30], S. Wenig[30], N. Wermes[21], M. Werner[48], P. Werner[30], M. Wessels[58a], J. Wetter[161], K. Whalen[116], A.M. Wharton[72], A. White[8], M.J. White[1], R. White[32b], S. White[124a,124b], D. Whiteson[163], F.J. Wickens[131], W. Wiedenmann[173], M. Wielers[131], P. Wienemann[21], C. Wiglesworth[36], L.A.M. Wiik-Fuchs[21], A. Wildauer[101], H.G. Wilkens[30], H.H. Williams[122], S. Williams[107], C. Willis[90], S. Willocq[86], A. Wilson[89], J.A. Wilson[18], I. Wingerter-Seez[5], F. Winklmeier[116], B.T. Winter[21], M. Wittgen[143], J. Wittkowski[100], S.J. Wollstadt[83], M.W. Wolter[39], H. Wolters[126a,126c], B.K. Wosiek[39], J. Wotschack[30], M.J. Woudstra[84], K.W. Wozniak[39], M. Wu[55], M. Wu[31], S.L. Wu[173], X. Wu[49], Y. Wu[89], T.R. Wyatt[84], B.M. Wynne[46], S. Xella[36], D. Xu[33a], L. Xu[33b,al], B. Yabsley[150], S. Yacoob[145b,am], R. Yakabe[67], M. Yamada[66], Y. Yamaguchi[118], A. Yamamoto[66], S. Yamamoto[155], T. Yamanaka[155], K. Yamauchi[103], Y. Yamazaki[67], Z. Yan[22], H. Yang[33e], H. Yang[173], Y. Yang[151], W-M. Yao[15], Y. Yasu[66], E. Yatsenko[5], K.H. Yau Wong[21], J. Ye[40], S. Ye[25], I. Yeletskikh[65], A.L. Yen[57], E. Yildirim[42], K. Yorita[171], R. Yoshida[6], K. Yoshihara[122], C. Young[143], C.J.S. Young[30], S. Youssef[22], D.R. Yu[15], J. Yu[8], J.M. Yu[89], J. Yu[114], L. Yuan[67], A. Yurkewicz[108], I. Yusuff[28,an], B. Zabinski[39], R. Zaidan[63], A.M. Zaitsev[130,ab], J. Zalieckas[14], A. Zaman[148], S. Zambito[57], L. Zanello[132a,132b], D. Zanzi[88], C. Zeitnitz[175], M. Zeman[128], A. Zemla[38a], K. Zengel[23], O. Zenin[130], T. Ženiš[144a], D. Zerwas[117], D. Zhang[89], F. Zhang[173], H. Zhang[33c], J. Zhang[6], L. Zhang[48], R. Zhang[33b], X. Zhang[33d], Z. Zhang[117], X. Zhao[40], Y. Zhao[33d,117], Z. Zhao[33b], A. Zhemchugov[65], J. Zhong[120], B. Zhou[89], C. Zhou[45], L. Zhou[35], L. Zhou[40], N. Zhou[163], C.G. Zhu[33d], H. Zhu[33a], J. Zhu[89], Y. Zhu[33b], X. Zhuang[33a], K. Zhukov[96], A. Zibell[174], D. Zieminska[61], N.I. Zimine[65], C. Zimmermann[83], S. Zimmermann[48], Z. Zinonos[54], M. Zinser[83], M. Ziolkowski[141], L. Živković[13], G. Zobernig[173], A. Zoccoli[20a,20b], M. zur Nedden[16], G. Zurzolo[104a,104b], L. Zwalinski[30].

[1] Department of Physics, University of Adelaide, Adelaide, Australia
[2] Physics Department, SUNY Albany, Albany NY, United States of America
[3] Department of Physics, University of Alberta, Edmonton AB, Canada
[4] (a) Department of Physics, Ankara University, Ankara; (b) Istanbul Aydin University, Istanbul; (c) Division of Physics, TOBB University of Economics and Technology, Ankara, Turkey
[5] LAPP, CNRS/IN2P3 and Université Savoie Mont Blanc, Annecy-le-Vieux, France
[6] High Energy Physics Division, Argonne National Laboratory, Argonne IL, United States of America
[7] Department of Physics, University of Arizona, Tucson AZ, United States of America
[8] Department of Physics, The University of Texas at Arlington, Arlington TX, United States of America

[9] Physics Department, University of Athens, Athens, Greece
[10] Physics Department, National Technical University of Athens, Zografou, Greece
[11] Institute of Physics, Azerbaijan Academy of Sciences, Baku, Azerbaijan
[12] Institut de Física d'Altes Energies (IFAE), The Barcelona Institute of Science and Technology, Barcelona, Spain, Spain
[13] Institute of Physics, University of Belgrade, Belgrade, Serbia
[14] Department for Physics and Technology, University of Bergen, Bergen, Norway
[15] Physics Division, Lawrence Berkeley National Laboratory and University of California, Berkeley CA, United States of America
[16] Department of Physics, Humboldt University, Berlin, Germany
[17] Albert Einstein Center for Fundamental Physics and Laboratory for High Energy Physics, University of Bern, Bern, Switzerland
[18] School of Physics and Astronomy, University of Birmingham, Birmingham, United Kingdom
[19] [(a)] Department of Physics, Bogazici University, Istanbul; [(b)] Department of Physics Engineering, Gaziantep University, Gaziantep; [(c)] Department of Physics, Dogus University, Istanbul, Turkey
[20] [(a)] INFN Sezione di Bologna; [(b)] Dipartimento di Fisica e Astronomia, Università di Bologna, Bologna, Italy
[21] Physikalisches Institut, University of Bonn, Bonn, Germany
[22] Department of Physics, Boston University, Boston MA, United States of America
[23] Department of Physics, Brandeis University, Waltham MA, United States of America
[24] [(a)] Universidade Federal do Rio De Janeiro COPPE/EE/IF, Rio de Janeiro; [(b)] Electrical Circuits Department, Federal University of Juiz de Fora (UFJF), Juiz de Fora; [(c)] Federal University of Sao Joao del Rei (UFSJ), Sao Joao del Rei; [(d)] Instituto de Fisica, Universidade de Sao Paulo, Sao Paulo, Brazil
[25] Physics Department, Brookhaven National Laboratory, Upton NY, United States of America
[26] [(a)] National Institute of Physics and Nuclear Engineering, Bucharest; [(b)] National Institute for Research and Development of Isotopic and Molecular Technologies, Physics Department, Cluj Napoca; [(c)] University Politehnica Bucharest, Bucharest; [(d)] West University in Timisoara, Timisoara, Romania
[27] Departamento de Física, Universidad de Buenos Aires, Buenos Aires, Argentina
[28] Cavendish Laboratory, University of Cambridge, Cambridge, United Kingdom
[29] Department of Physics, Carleton University, Ottawa ON, Canada
[30] CERN, Geneva, Switzerland
[31] Enrico Fermi Institute, University of Chicago, Chicago IL, United States of America
[32] [(a)] Departamento de Física, Pontificia Universidad Católica de Chile, Santiago; [(b)] Departamento de Física, Universidad Técnica Federico Santa María, Valparaíso, Chile
[33] [(a)] Institute of High Energy Physics, Chinese Academy of Sciences, Beijing; [(b)] Department of Modern Physics, University of Science and Technology of China, Anhui; [(c)] Department of Physics, Nanjing University, Jiangsu; [(d)] School of Physics, Shandong University, Shandong; [(e)] Department of Physics and Astronomy, Shanghai Key Laboratory for Particle Physics and Cosmology, Shanghai Jiao Tong University, Shanghai; [(f)] Physics Department, Tsinghua University, Beijing 100084, China
[34] Laboratoire de Physique Corpusculaire, Clermont Université and Université Blaise Pascal and CNRS/IN2P3, Clermont-Ferrand, France
[35] Nevis Laboratory, Columbia University, Irvington NY, United States of America
[36] Niels Bohr Institute, University of Copenhagen, Kobenhavn, Denmark
[37] [(a)] INFN Gruppo Collegato di Cosenza, Laboratori Nazionali di Frascati; [(b)] Dipartimento di Fisica, Università della Calabria, Rende, Italy
[38] [(a)] AGH University of Science and Technology, Faculty of Physics and Applied Computer Science, Krakow; [(b)] Marian Smoluchowski Institute of Physics, Jagiellonian University, Krakow, Poland

[39] Institute of Nuclear Physics Polish Academy of Sciences, Krakow, Poland
[40] Physics Department, Southern Methodist University, Dallas TX, United States of America
[41] Physics Department, University of Texas at Dallas, Richardson TX, United States of America
[42] DESY, Hamburg and Zeuthen, Germany
[43] Institut für Experimentelle Physik IV, Technische Universität Dortmund, Dortmund, Germany
[44] Institut für Kern- und Teilchenphysik, Technische Universität Dresden, Dresden, Germany
[45] Department of Physics, Duke University, Durham NC, United States of America
[46] SUPA - School of Physics and Astronomy, University of Edinburgh, Edinburgh, United Kingdom
[47] INFN Laboratori Nazionali di Frascati, Frascati, Italy
[48] Fakultät für Mathematik und Physik, Albert-Ludwigs-Universität, Freiburg, Germany
[49] Section de Physique, Université de Genève, Geneva, Switzerland
[50] [(a)] INFN Sezione di Genova; [(b)] Dipartimento di Fisica, Università di Genova, Genova, Italy
[51] [(a)] E. Andronikashvili Institute of Physics, Iv. Javakhishvili Tbilisi State University, Tbilisi; [(b)] High Energy Physics Institute, Tbilisi State University, Tbilisi, Georgia
[52] II Physikalisches Institut, Justus-Liebig-Universität Giessen, Giessen, Germany
[53] SUPA - School of Physics and Astronomy, University of Glasgow, Glasgow, United Kingdom
[54] II Physikalisches Institut, Georg-August-Universität, Göttingen, Germany
[55] Laboratoire de Physique Subatomique et de Cosmologie, Université Grenoble-Alpes, CNRS/IN2P3, Grenoble, France
[56] Department of Physics, Hampton University, Hampton VA, United States of America
[57] Laboratory for Particle Physics and Cosmology, Harvard University, Cambridge MA, United States of America
[58] [(a)] Kirchhoff-Institut für Physik, Ruprecht-Karls-Universität Heidelberg, Heidelberg; [(b)] Physikalisches Institut, Ruprecht-Karls-Universität Heidelberg, Heidelberg; [(c)] ZITI Institut für technische Informatik, Ruprecht-Karls-Universität Heidelberg, Mannheim, Germany
[59] Faculty of Applied Information Science, Hiroshima Institute of Technology, Hiroshima, Japan
[60] [(a)] Department of Physics, The Chinese University of Hong Kong, Shatin, N.T., Hong Kong; [(b)] Department of Physics, The University of Hong Kong, Hong Kong; [(c)] Department of Physics, The Hong Kong University of Science and Technology, Clear Water Bay, Kowloon, Hong Kong, China
[61] Department of Physics, Indiana University, Bloomington IN, United States of America
[62] Institut für Astro- und Teilchenphysik, Leopold-Franzens-Universität, Innsbruck, Austria
[63] University of Iowa, Iowa City IA, United States of America
[64] Department of Physics and Astronomy, Iowa State University, Ames IA, United States of America
[65] Joint Institute for Nuclear Research, JINR Dubna, Dubna, Russia
[66] KEK, High Energy Accelerator Research Organization, Tsukuba, Japan
[67] Graduate School of Science, Kobe University, Kobe, Japan
[68] Faculty of Science, Kyoto University, Kyoto, Japan
[69] Kyoto University of Education, Kyoto, Japan
[70] Department of Physics, Kyushu University, Fukuoka, Japan
[71] Instituto de Física La Plata, Universidad Nacional de La Plata and CONICET, La Plata, Argentina
[72] Physics Department, Lancaster University, Lancaster, United Kingdom
[73] [(a)] INFN Sezione di Lecce; [(b)] Dipartimento di Matematica e Fisica, Università del Salento, Lecce, Italy
[74] Oliver Lodge Laboratory, University of Liverpool, Liverpool, United Kingdom
[75] Department of Physics, Jožef Stefan Institute and University of Ljubljana, Ljubljana, Slovenia
[76] School of Physics and Astronomy, Queen Mary University of London, London, United Kingdom
[77] Department of Physics, Royal Holloway University of London, Surrey, United Kingdom

[78] Department of Physics and Astronomy, University College London, London, United Kingdom
[79] Louisiana Tech University, Ruston LA, United States of America
[80] Laboratoire de Physique Nucléaire et de Hautes Energies, UPMC and Université Paris-Diderot and CNRS/IN2P3, Paris, France
[81] Fysiska institutionen, Lunds universitet, Lund, Sweden
[82] Departamento de Fisica Teorica C-15, Universidad Autonoma de Madrid, Madrid, Spain
[83] Institut für Physik, Universität Mainz, Mainz, Germany
[84] School of Physics and Astronomy, University of Manchester, Manchester, United Kingdom
[85] CPPM, Aix-Marseille Université and CNRS/IN2P3, Marseille, France
[86] Department of Physics, University of Massachusetts, Amherst MA, United States of America
[87] Department of Physics, McGill University, Montreal QC, Canada
[88] School of Physics, University of Melbourne, Victoria, Australia
[89] Department of Physics, The University of Michigan, Ann Arbor MI, United States of America
[90] Department of Physics and Astronomy, Michigan State University, East Lansing MI, United States of America
[91] [(a)] INFN Sezione di Milano; [(b)] Dipartimento di Fisica, Università di Milano, Milano, Italy
[92] B.I. Stepanov Institute of Physics, National Academy of Sciences of Belarus, Minsk, Republic of Belarus
[93] National Scientific and Educational Centre for Particle and High Energy Physics, Minsk, Republic of Belarus
[94] Department of Physics, Massachusetts Institute of Technology, Cambridge MA, United States of America
[95] Group of Particle Physics, University of Montreal, Montreal QC, Canada
[96] P.N. Lebedev Physical Institute of the Russian Academy of Sciences, Moscow, Russia
[97] Institute for Theoretical and Experimental Physics (ITEP), Moscow, Russia
[98] National Research Nuclear University MEPhI, Moscow, Russia
[99] D.V. Skobeltsyn Institute of Nuclear Physics, M.V. Lomonosov Moscow State University, Moscow, Russia
[100] Fakultät für Physik, Ludwig-Maximilians-Universität München, München, Germany
[101] Max-Planck-Institut für Physik (Werner-Heisenberg-Institut), München, Germany
[102] Nagasaki Institute of Applied Science, Nagasaki, Japan
[103] Graduate School of Science and Kobayashi-Maskawa Institute, Nagoya University, Nagoya, Japan
[104] [(a)] INFN Sezione di Napoli; [(b)] Dipartimento di Fisica, Università di Napoli, Napoli, Italy
[105] Department of Physics and Astronomy, University of New Mexico, Albuquerque NM, United States of America
[106] Institute for Mathematics, Astrophysics and Particle Physics, Radboud University Nijmegen/Nikhef, Nijmegen, Netherlands
[107] Nikhef National Institute for Subatomic Physics and University of Amsterdam, Amsterdam, Netherlands
[108] Department of Physics, Northern Illinois University, DeKalb IL, United States of America
[109] Budker Institute of Nuclear Physics, SB RAS, Novosibirsk, Russia
[110] Department of Physics, New York University, New York NY, United States of America
[111] Ohio State University, Columbus OH, United States of America
[112] Faculty of Science, Okayama University, Okayama, Japan
[113] Homer L. Dodge Department of Physics and Astronomy, University of Oklahoma, Norman OK, United States of America
[114] Department of Physics, Oklahoma State University, Stillwater OK, United States of America

[115] Palacký University, RCPTM, Olomouc, Czech Republic
[116] Center for High Energy Physics, University of Oregon, Eugene OR, United States of America
[117] LAL, Univ. Paris-Sud, CNRS/IN2P3, Université Paris-Saclay, Orsay, France
[118] Graduate School of Science, Osaka University, Osaka, Japan
[119] Department of Physics, University of Oslo, Oslo, Norway
[120] Department of Physics, Oxford University, Oxford, United Kingdom
[121] [(a)] INFN Sezione di Pavia; [(b)] Dipartimento di Fisica, Università di Pavia, Pavia, Italy
[122] Department of Physics, University of Pennsylvania, Philadelphia PA, United States of America
[123] National Research Centre "Kurchatov Institute" B.P.Konstantinov Petersburg Nuclear Physics Institute, St. Petersburg, Russia
[124] [(a)] INFN Sezione di Pisa; [(b)] Dipartimento di Fisica E. Fermi, Università di Pisa, Pisa, Italy
[125] Department of Physics and Astronomy, University of Pittsburgh, Pittsburgh PA, United States of America
[126] [(a)] Laboratório de Instrumentação e Física Experimental de Partículas - LIP, Lisboa; [(b)] Faculdade de Ciências, Universidade de Lisboa, Lisboa; [(c)] Department of Physics, University of Coimbra, Coimbra; [(d)] Centro de Física Nuclear da Universidade de Lisboa, Lisboa; [(e)] Departamento de Fisica, Universidade do Minho, Braga; [(f)] Departamento de Fisica Teorica y del Cosmos and CAFPE, Universidad de Granada, Granada (Spain); [(g)] Dep Fisica and CEFITEC of Faculdade de Ciencias e Tecnologia, Universidade Nova de Lisboa, Caparica, Portugal
[127] Institute of Physics, Academy of Sciences of the Czech Republic, Praha, Czech Republic
[128] Czech Technical University in Prague, Praha, Czech Republic
[129] Faculty of Mathematics and Physics, Charles University in Prague, Praha, Czech Republic
[130] State Research Center Institute for High Energy Physics (Protvino), NRC KI,Russia, Russia
[131] Particle Physics Department, Rutherford Appleton Laboratory, Didcot, United Kingdom
[132] [(a)] INFN Sezione di Roma; [(b)] Dipartimento di Fisica, Sapienza Università di Roma, Roma, Italy
[133] [(a)] INFN Sezione di Roma Tor Vergata; [(b)] Dipartimento di Fisica, Università di Roma Tor Vergata, Roma, Italy
[134] [(a)] INFN Sezione di Roma Tre; [(b)] Dipartimento di Matematica e Fisica, Università Roma Tre, Roma, Italy
[135] [(a)] Faculté des Sciences Ain Chock, Réseau Universitaire de Physique des Hautes Energies - Université Hassan II, Casablanca; [(b)] Centre National de l'Energie des Sciences Techniques Nucleaires, Rabat; [(c)] Faculté des Sciences Semlalia, Université Cadi Ayyad, LPHEA-Marrakech; [(d)] Faculté des Sciences, Université Mohamed Premier and LPTPM, Oujda; [(e)] Faculté des sciences, Université Mohammed V, Rabat, Morocco
[136] DSM/IRFU (Institut de Recherches sur les Lois Fondamentales de l'Univers), CEA Saclay (Commissariat à l'Energie Atomique et aux Energies Alternatives), Gif-sur-Yvette, France
[137] Santa Cruz Institute for Particle Physics, University of California Santa Cruz, Santa Cruz CA, United States of America
[138] Department of Physics, University of Washington, Seattle WA, United States of America
[139] Department of Physics and Astronomy, University of Sheffield, Sheffield, United Kingdom
[140] Department of Physics, Shinshu University, Nagano, Japan
[141] Fachbereich Physik, Universität Siegen, Siegen, Germany
[142] Department of Physics, Simon Fraser University, Burnaby BC, Canada
[143] SLAC National Accelerator Laboratory, Stanford CA, United States of America
[144] [(a)] Faculty of Mathematics, Physics & Informatics, Comenius University, Bratislava; [(b)] Department of Subnuclear Physics, Institute of Experimental Physics of the Slovak Academy of Sciences, Kosice, Slovak Republic

[145] [(a)] Department of Physics, University of Cape Town, Cape Town; [(b)] Department of Physics, University of Johannesburg, Johannesburg; [(c)] School of Physics, University of the Witwatersrand, Johannesburg, South Africa
[146] [(a)] Department of Physics, Stockholm University; [(b)] The Oskar Klein Centre, Stockholm, Sweden
[147] Physics Department, Royal Institute of Technology, Stockholm, Sweden
[148] Departments of Physics & Astronomy and Chemistry, Stony Brook University, Stony Brook NY, United States of America
[149] Department of Physics and Astronomy, University of Sussex, Brighton, United Kingdom
[150] School of Physics, University of Sydney, Sydney, Australia
[151] Institute of Physics, Academia Sinica, Taipei, Taiwan
[152] Department of Physics, Technion: Israel Institute of Technology, Haifa, Israel
[153] Raymond and Beverly Sackler School of Physics and Astronomy, Tel Aviv University, Tel Aviv, Israel
[154] Department of Physics, Aristotle University of Thessaloniki, Thessaloniki, Greece
[155] International Center for Elementary Particle Physics and Department of Physics, The University of Tokyo, Tokyo, Japan
[156] Graduate School of Science and Technology, Tokyo Metropolitan University, Tokyo, Japan
[157] Department of Physics, Tokyo Institute of Technology, Tokyo, Japan
[158] Department of Physics, University of Toronto, Toronto ON, Canada
[159] [(a)] TRIUMF, Vancouver BC; [(b)] Department of Physics and Astronomy, York University, Toronto ON, Canada
[160] Faculty of Pure and Applied Sciences, and Center for Integrated Research in Fundamental Science and Engineering, University of Tsukuba, Tsukuba, Japan
[161] Department of Physics and Astronomy, Tufts University, Medford MA, United States of America
[162] Centro de Investigaciones, Universidad Antonio Narino, Bogota, Colombia
[163] Department of Physics and Astronomy, University of California Irvine, Irvine CA, United States of America
[164] [(a)] INFN Gruppo Collegato di Udine, Sezione di Trieste, Udine; [(b)] ICTP, Trieste; [(c)] Dipartimento di Chimica, Fisica e Ambiente, Università di Udine, Udine, Italy
[165] Department of Physics, University of Illinois, Urbana IL, United States of America
[166] Department of Physics and Astronomy, University of Uppsala, Uppsala, Sweden
[167] Instituto de Física Corpuscular (IFIC) and Departamento de Física Atómica, Molecular y Nuclear and Departamento de Ingeniería Electrónica and Instituto de Microelectrónica de Barcelona (IMB-CNM), University of Valencia and CSIC, Valencia, Spain
[168] Department of Physics, University of British Columbia, Vancouver BC, Canada
[169] Department of Physics and Astronomy, University of Victoria, Victoria BC, Canada
[170] Department of Physics, University of Warwick, Coventry, United Kingdom
[171] Waseda University, Tokyo, Japan
[172] Department of Particle Physics, The Weizmann Institute of Science, Rehovot, Israel
[173] Department of Physics, University of Wisconsin, Madison WI, United States of America
[174] Fakultät für Physik und Astronomie, Julius-Maximilians-Universität, Würzburg, Germany
[175] Fakult[̈a]t für Mathematik und Naturwissenschaften, Fachgruppe Physik, Bergische Universität Wuppertal, Wuppertal, Germany
[176] Department of Physics, Yale University, New Haven CT, United States of America
[177] Yerevan Physics Institute, Yerevan, Armenia
[178] Centre de Calcul de l'Institut National de Physique Nucléaire et de Physique des Particules (IN2P3), Villeurbanne, France

[a] Also at Department of Physics, King's College London, London, United Kingdom
[b] Also at Institute of Physics, Azerbaijan Academy of Sciences, Baku, Azerbaijan
[c] Also at Novosibirsk State University, Novosibirsk, Russia
[d] Also at TRIUMF, Vancouver BC, Canada
[e] Also at Department of Physics, California State University, Fresno CA, United States of America
[f] Also at Department of Physics, University of Fribourg, Fribourg, Switzerland
[g] Also at Departamento de Fisica e Astronomia, Faculdade de Ciencias, Universidade do Porto, Portugal
[h] Also at Tomsk State University, Tomsk, Russia
[i] Also at CPPM, Aix-Marseille Université and CNRS/IN2P3, Marseille, France
[j] Also at Universita di Napoli Parthenope, Napoli, Italy
[k] Also at Institute of Particle Physics (IPP), Canada
[l] Also at Particle Physics Department, Rutherford Appleton Laboratory, Didcot, United Kingdom
[m] Also at Department of Physics, St. Petersburg State Polytechnical University, St. Petersburg, Russia
[n] Also at Louisiana Tech University, Ruston LA, United States of America
[o] Also at Institucio Catalana de Recerca i Estudis Avancats, ICREA, Barcelona, Spain
[p] Also at Department of Physics, National Tsing Hua University, Taiwan
[q] Also at Department of Physics, The University of Texas at Austin, Austin TX, United States of America
[r] Also at Institute of Theoretical Physics, Ilia State University, Tbilisi, Georgia
[s] Also at CERN, Geneva, Switzerland
[t] Also at Georgian Technical University (GTU),Tbilisi, Georgia
[u] Also at Ochadai Academic Production, Ochanomizu University, Tokyo, Japan
[v] Also at Manhattan College, New York NY, United States of America
[w] Also at Hellenic Open University, Patras, Greece
[x] Also at Institute of Physics, Academia Sinica, Taipei, Taiwan
[y] Also at LAL, Univ. Paris-Sud, CNRS/IN2P3, Université Paris-Saclay, Orsay, France
[z] Also at Academia Sinica Grid Computing, Institute of Physics, Academia Sinica, Taipei, Taiwan
[aa] Also at School of Physics, Shandong University, Shandong, China
[ab] Also at Moscow Institute of Physics and Technology State University, Dolgoprudny, Russia
[ac] Also at Section de Physique, Université de Genève, Geneva, Switzerland
[ad] Also at International School for Advanced Studies (SISSA), Trieste, Italy
[ae] Also at Department of Physics and Astronomy, University of South Carolina, Columbia SC, United States of America
[af] Also at School of Physics and Engineering, Sun Yat-sen University, Guangzhou, China
[ag] Also at Faculty of Physics, M.V.Lomonosov Moscow State University, Moscow, Russia
[ah] Also at National Research Nuclear University MEPhI, Moscow, Russia
[ai] Also at Department of Physics, Stanford University, Stanford CA, United States of America
[aj] Also at Institute for Particle and Nuclear Physics, Wigner Research Centre for Physics, Budapest, Hungary
[ak] Also at Flensburg University of Applied Sciences, Flensburg, Germany
[al] Also at Department of Physics, The University of Michigan, Ann Arbor MI, United States of America
[am] Also at Discipline of Physics, University of KwaZulu-Natal, Durban, South Africa
[an] Also at University of Malaya, Department of Physics, Kuala Lumpur, Malaysia
* Deceased